N^* Spectroscopy from Lattice QCD

Derek Leinweber

Special Research Centre for the Subatomic Structure of Matter

The University of Adelaide

Baryon Spectrum: Hadron Spectrum Collaboration

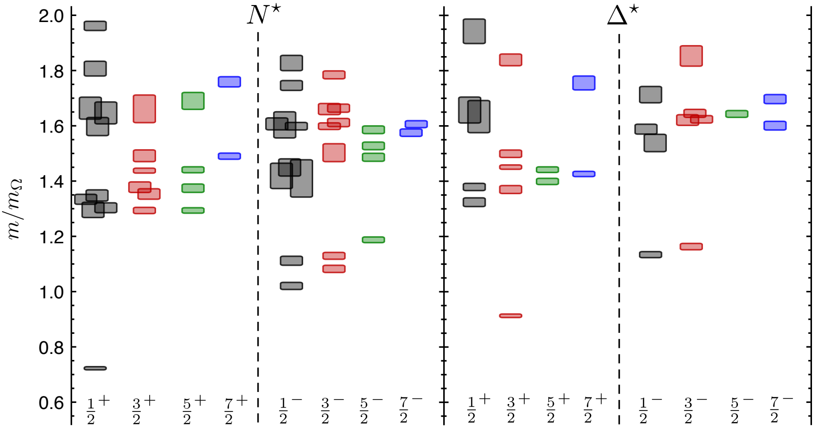

Positive Parity Nucleon Spectrum: χQCD (U. Kentucky) Collaboration

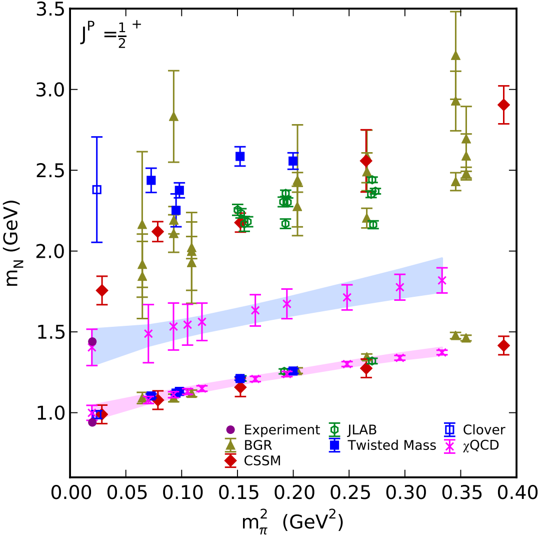

Positive Parity Spectrum: Cypress (Twisted Mass) Collaboration: Feb. '13

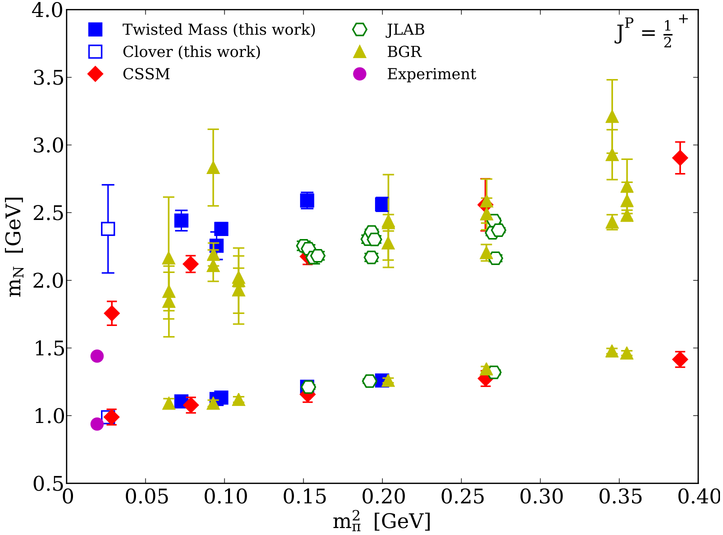

Positive Parity Spectrum: Cypress (Twisted Mass) Collaboration: Jan. '14

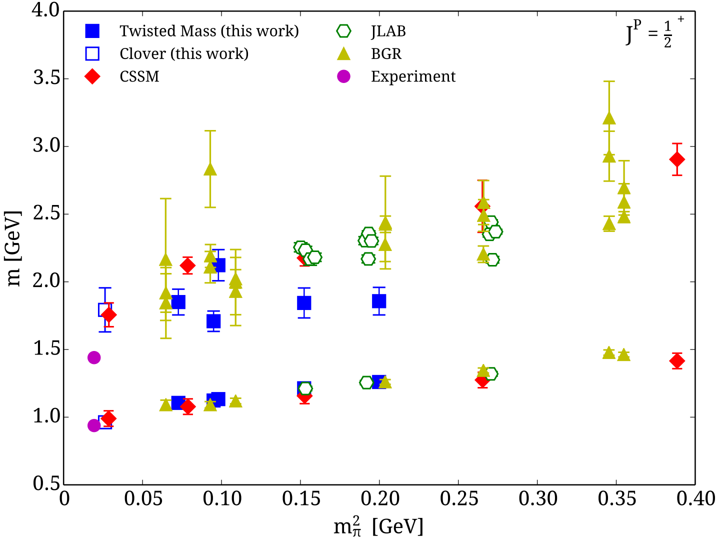

Negative Parity Nucleon Spectrum: Cypress

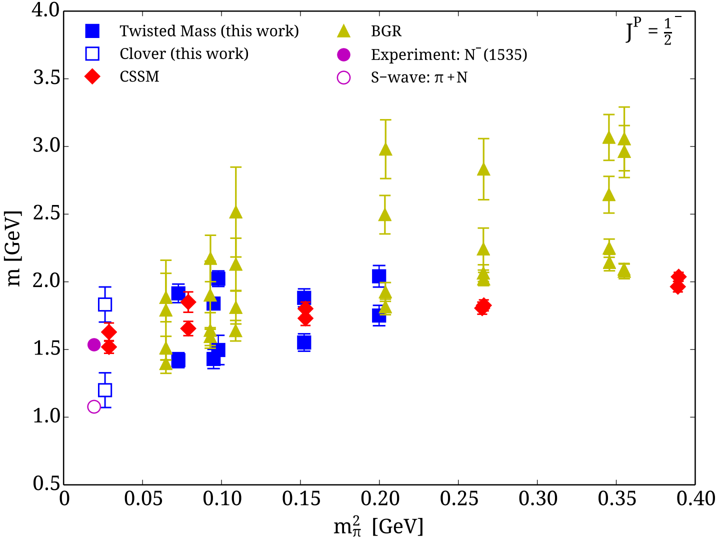

Outline

Variational Analysis

- Consider a basis of interpolating fields χ_i

Variational Analysis

- Consider a basis of interpolating fields χ_i
- Construct the correlation matrix

$$G_{ij}(\mathbf{p};t) = \sum_{\mathbf{x}} \mathrm{e}^{-\mathrm{i}\,\mathbf{p}\cdot\mathbf{x}}\, \mathrm{tr}\left(\Gamma\, \langle\Omega|\, \chi_i(x)\, \overline{\chi}_j(0)\, |\Omega\rangle \right).$$

Variational Analysis

- Consider a basis of interpolating fields χ_i
- Construct the correlation matrix

$$G_{ij}(\mathbf{p};t) = \sum_{\mathbf{x}} \mathrm{e}^{-\mathrm{i}\,\mathbf{p}\cdot\mathbf{x}}\, \mathrm{tr}\left(\, \Gamma\, \langle\Omega|\, \chi_i(x)\, \overline{\chi}_j(0)\, |\Omega\rangle \,\right).$$

- Seek linear combinations of the interpolators $\{\, \chi_i \,\}$ that isolate individual energy eigenstates, α, at momentum $\mathbf{p}$:

$$\phi^\alpha = v_i^\alpha(\mathbf{p})\, \chi_i\,, \qquad \overline{\phi}^\alpha = u_i^\alpha(\mathbf{p})\, \overline{\chi}_i\,.$$

Variational Analysis

- When successful, only state α participates in the correlation function, and one can write recurrence relations

$$G(\mathbf{p}; t_0 + \delta t)\, \mathbf{u}^{\alpha}(\mathbf{p}) = \mathrm{e}^{-E_\alpha(\mathbf{p})\,\delta t}\, G(\mathbf{p}; t_0)\, \mathbf{u}^{\alpha}(\mathbf{p})$$

$$\mathbf{v}^{\alpha\mathsf{T}}(\mathbf{p})\, G(\mathbf{p}; t_0 + \delta t) = \mathrm{e}^{-E_\alpha(\mathbf{p})\,\delta t}\, \mathbf{v}^{\alpha\mathsf{T}}(\mathbf{p})\, G(\mathbf{p}; t_0)$$

a Generalised Eigenvalue Problem (GEVP).

Variational Analysis

- When successful, only state α participates in the correlation function, and one can write recurrence relations

$$G(\mathbf{p}; t_0 + \delta t)\, \mathbf{u}^{\alpha}(\mathbf{p}) = \mathrm{e}^{-E_\alpha(\mathbf{p})\,\delta t}\, G(\mathbf{p}; t_0)\, \mathbf{u}^{\alpha}(\mathbf{p})$$

$$\mathbf{v}^{\alpha\mathsf{T}}(\mathbf{p})\, G(\mathbf{p}; t_0 + \delta t) = \mathrm{e}^{-E_\alpha(\mathbf{p})\,\delta t}\, \mathbf{v}^{\alpha\mathsf{T}}(\mathbf{p})\, G(\mathbf{p}; t_0)$$

  a Generalised Eigenvalue Problem (GEVP).
- Solve for the left, $\mathbf{v}^{\alpha}(\mathbf{p})$, and right, $\mathbf{u}^{\alpha}(\mathbf{p})$, generalised eigenvectors of $G(\mathbf{p}; t_0 + \delta t)$ and $G(\mathbf{p}; t_0)$.

Eigenstate-Projected Correlation Functions

- Using these optimal eigenvectors, create eigenstate-projected correlation functions

$$\begin{aligned} G^{\alpha}(\mathbf{p};t) &= \sum_{\mathbf{x}} \mathrm{e}^{-\mathrm{i}\,\mathbf{p}\cdot\mathbf{x}} \, \langle\Omega|\phi^{\alpha}(x)\,\overline{\phi}^{\alpha}(0)|\Omega\rangle \ , \\ &= \sum_{\mathbf{x}} \mathrm{e}^{-\mathrm{i}\,\mathbf{p}\cdot\mathbf{x}} \, \langle\Omega|v_i^{\alpha}(\mathbf{p})\,\chi_i(x)\,\overline{\chi}_j(0)\,u_j^{\alpha}(\mathbf{p})|\Omega\rangle \ , \\ &= \mathbf{v}^{\alpha\mathsf{T}}(\mathbf{p})\,G(\mathbf{p};t)\,\mathbf{u}^{\alpha}(\mathbf{p})\,. \end{aligned}$$

$$G^{\alpha}(\mathbf{p};t) = A_{\alpha}\,\exp\left(-E_{\alpha}(\mathbf{p})\,t\right) \ .$$

Eigenstate-Projected Correlation Functions

- Using these optimal eigenvectors, create eigenstate-projected correlation functions

$$
\begin{aligned}
G^\alpha(\mathbf{p};t) &= \sum_{\mathbf{x}} \mathrm{e}^{-\mathrm{i}\,\mathbf{p}\cdot\mathbf{x}} \, \langle \Omega | \phi^\alpha(x)\, \overline{\phi}^\alpha(0) | \Omega \rangle \ , \\
&= \sum_{\mathbf{x}} \mathrm{e}^{-\mathrm{i}\,\mathbf{p}\cdot\mathbf{x}} \, \langle \Omega | v_i^\alpha(\mathbf{p})\, \chi_i(x)\, \overline{\chi}_j(0)\, u_j^\alpha(\mathbf{p}) | \Omega \rangle \ , \\
&= \mathbf{v}^{\alpha\,\mathsf{T}}(\mathbf{p})\, G(\mathbf{p};t)\, \mathbf{u}^\alpha(\mathbf{p})\, .
\end{aligned}
$$

$$
G^\alpha(\mathbf{p};t) = A_\alpha \, \exp\left(-E_\alpha(\mathbf{p})\, t\right) \ .
$$

- Here t is different from t_0 and δt and can become large.

Defining the Effective Mass

- At zero momentum, the projected correlator is

$$G^{\alpha}(\mathbf{0};t) = A_{\alpha}\,\exp\left(-M_{\alpha}\,t\right)\,.$$

Defining the Effective Mass

- At zero momentum, the projected correlator is

$$G^{\alpha}(\mathbf{0};t) = A_\alpha \exp\left(-M_\alpha\, t\right) \,.$$

- Taking the log

$$\ln G^{\alpha}(\mathbf{0};t) = \ln\left(A_\alpha\right) - M_\alpha\, t \,.$$

Defining the Effective Mass

- At zero momentum, the projected correlator is

$$G^{\alpha}(\mathbf{0};t) = A_{\alpha}\,\exp\left(-M_{\alpha}\,t\right)\ .$$

- Taking the log

$$\ln G^{\alpha}(\mathbf{0};t) = \ln\left(A_{\alpha}\right) - M_{\alpha}\,t\,.$$

- The effective mass is defined as

$$M^{\alpha}_{\rm eff}(t) = \frac{1}{\Delta t}\ln\left(\frac{G^{\alpha}(t)}{G^{\alpha}(t+\Delta t)}\right)\ .$$

Defining the Effective Mass

- At zero momentum, the projected correlator is

$$G^{\alpha}(\mathbf{0};t) = A_{\alpha}\, \exp\left(-M_{\alpha}\, t\right)\ .$$

- Taking the log

$$\ln G^{\alpha}(\mathbf{0};t) = \ln\left(A_{\alpha}\right) - M_{\alpha}\, t\,.$$

- The effective mass is defined as

$$M^{\alpha}_{\mathrm{eff}}(t) = \frac{1}{\Delta t} \ln\left(\frac{G^{\alpha}(t)}{G^{\alpha}(t+\Delta t)}\right)\ .$$

- $\Delta t = 1$ or 2 is common.

Smeared Source to Point Sink Correlation Functions

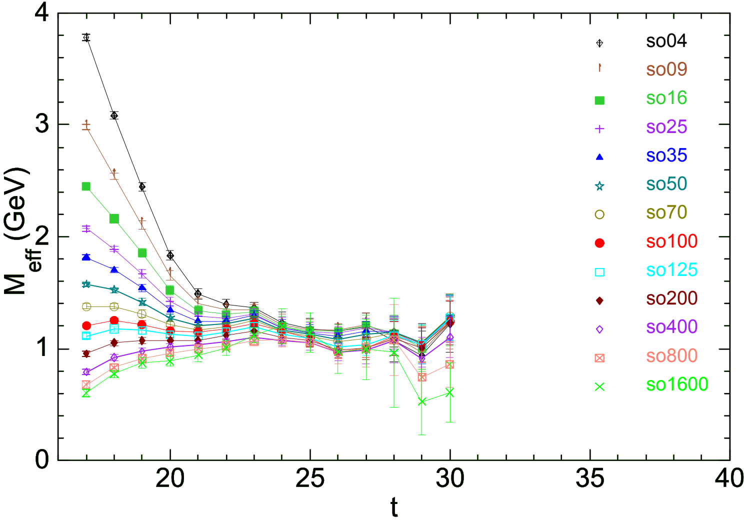

Positive Parity Nucleon - First Excited State - m_π: 296 MeV

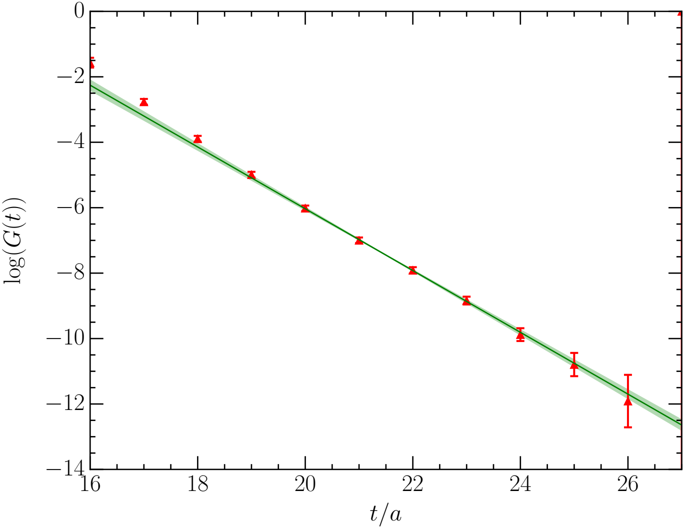

Positive Parity Nucleon - First Excited State - m_π: 296 MeV - χ^2_{dof}: 0.67

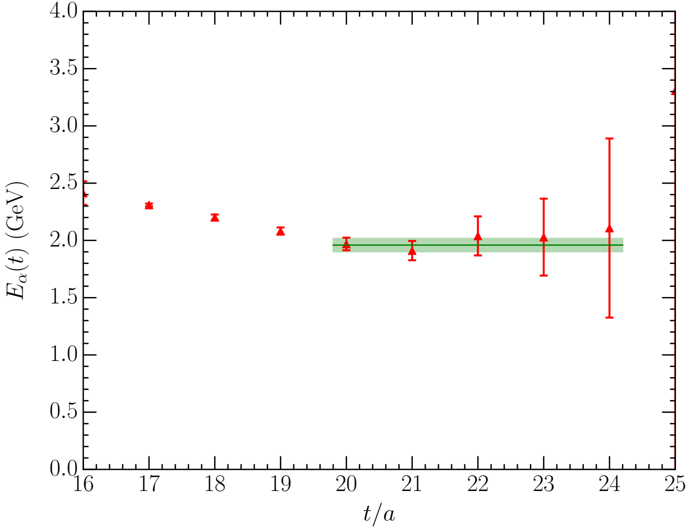

Negative Parity Nucleon - 2nd Excited State - m_π: 156 MeV

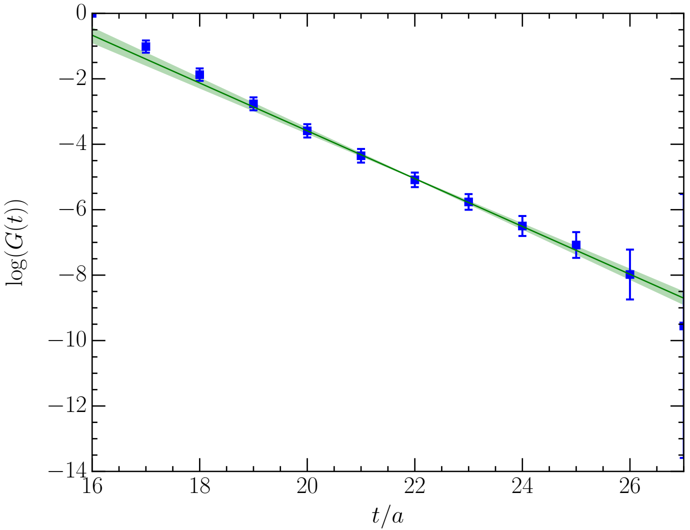

Negative Parity Nucleon - 2nd Excited State - m_π: 156 MeV - χ^2_{dof}: 0.88

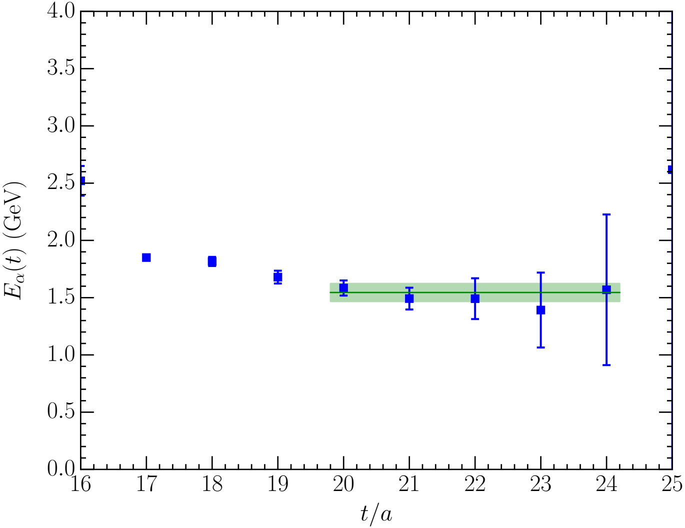

Further Information

- "Roper Resonance in 2+1 Flavor QCD,"
  M. S. Mahbub, *et al.* [CSSM],
  Phys. Lett. B **707** (2012) 389
  arXiv:1011.5724 [hep-lat],

- "Low-lying Odd-parity States of the Nucleon in Lattice QCD,"
  M. Selim Mahbub, *et al.* [CSSM],
  Phys. Rev. D Rapid Comm. **87** (2013) 011501,
  arXiv:1209.0240 [hep-lat]

- "Structure and Flow of the Nucleon Eigenstates in Lattice QCD,"
  M. S. Mahbub, *et al.* [CSSM],
  Phys. Rev. D **87** (2013) 9, 094506
  arXiv:1302.2987 [hep-lat].

- Finn Stokes, *et al.* [CSSM], In preparation.

CSSM Simulation Details

Based on the PACS-CS $(2+1)$-flavour ensembles, available through the ILDG.

S. Aoki *et al* (PACS-CS Collaboration), Phys. Rev. D **79**, 034503 (2009)

- Lattice size of $32^3 \times 64$ with $\beta = 1.90$. $L \simeq 3$ fm.

CSSM Simulation Details

Based on the PACS-CS $(2+1)$-flavour ensembles, available through the ILDG.

S. Aoki *et al* (PACS-CS Collaboration), Phys. Rev. D **79**, 034503 (2009)

- Lattice size of $32^3 \times 64$ with $\beta = 1.90$. $L \simeq 3$ fm.
- 5 pion masses, ranging from 640 MeV down to 156 MeV.

CSSM Simulation Details

Based on the PACS-CS $(2+1)$-flavour ensembles, available through the ILDG.

S. Aoki *et al* (PACS-CS Collaboration), Phys. Rev. D **79**, 034503 (2009)

- Lattice size of $32^3 \times 64$ with $\beta = 1.90$. $L \simeq 3$ fm.
- 5 pion masses, ranging from 640 MeV down to 156 MeV.
- The strange quark κ_s is held fixed as the light quark masses vary.
  - Changes in the strange quark contributions are environmental effects.

Positive Parity Nucleon Spectrum: CSSM

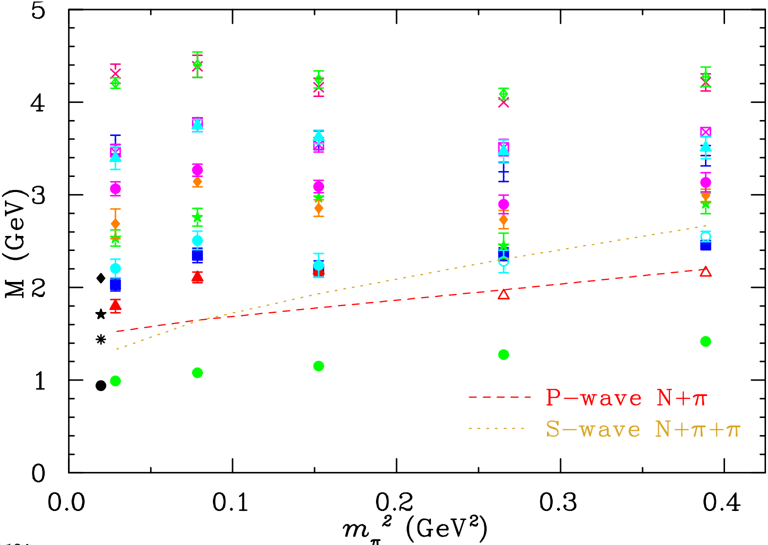

States Tracked via Orthogonal Eigenvectors

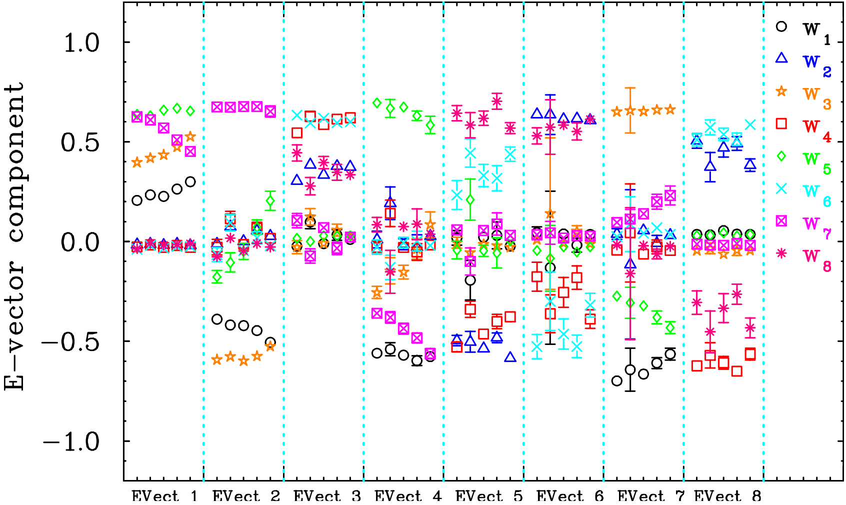

Positive Parity Nucleon Spectrum: CSSM

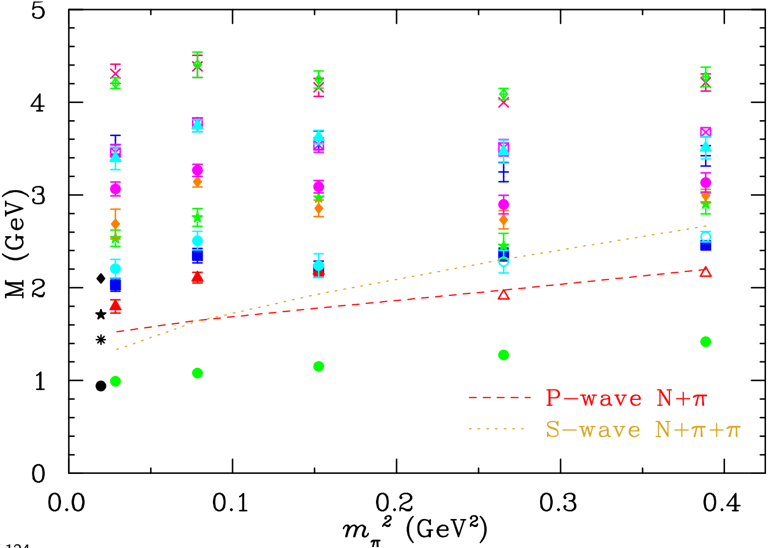

Comparison: Hadron Spectrum Collaboration (HSC)

- "Excited state baryon spectroscopy from lattice QCD," R. G. Edwards, J. J. Dudek, D. G. Richards and S. J. Wallace, Phys. Rev. D **84** (2011) 074508 arXiv:1104.5152 [hep-ph].

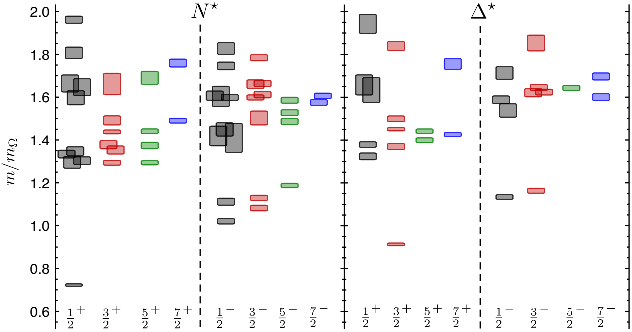

CSSM & HSC Comparison: Positive Parity CSSM

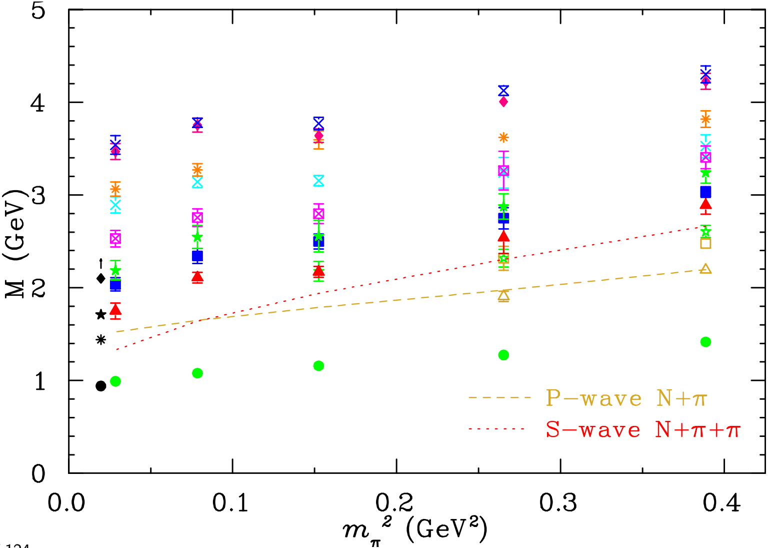

CSSM & HSC Comparison: Positive Parity CSSM

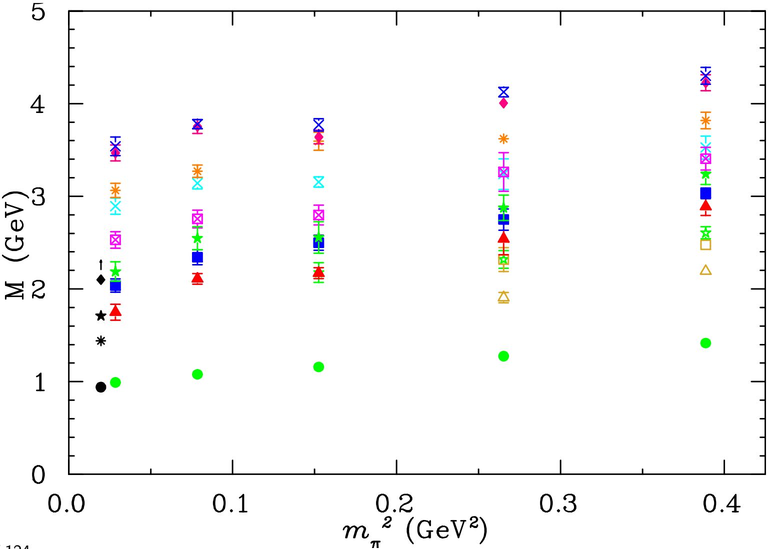

CSSM & HSC Comparison: Positive Parity

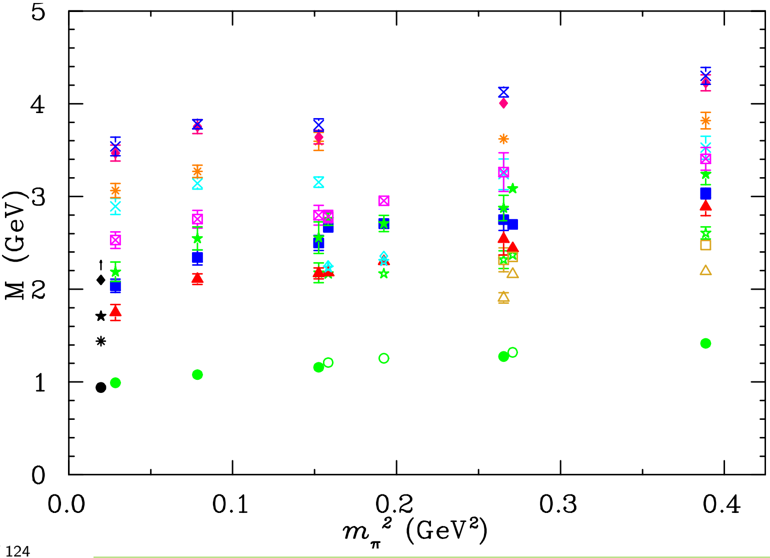

CSSM & HSC Comparison: Negative Parity CSSM

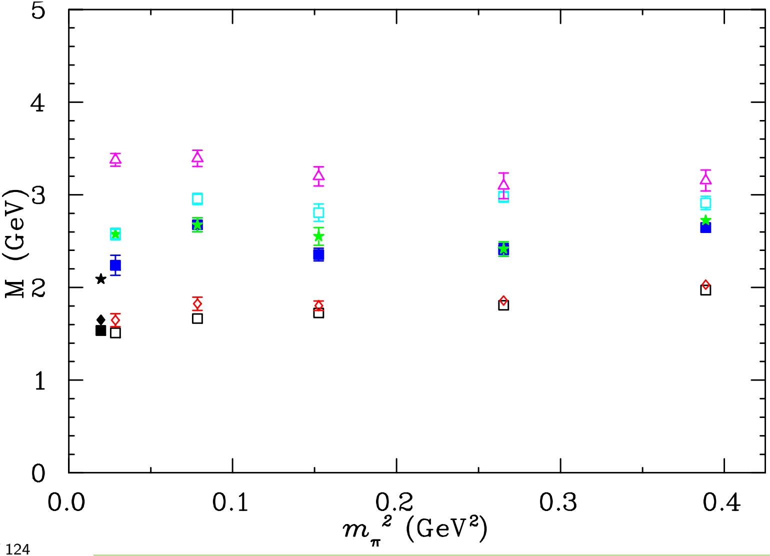

CSSM & HSC Comparison: Negative Parity

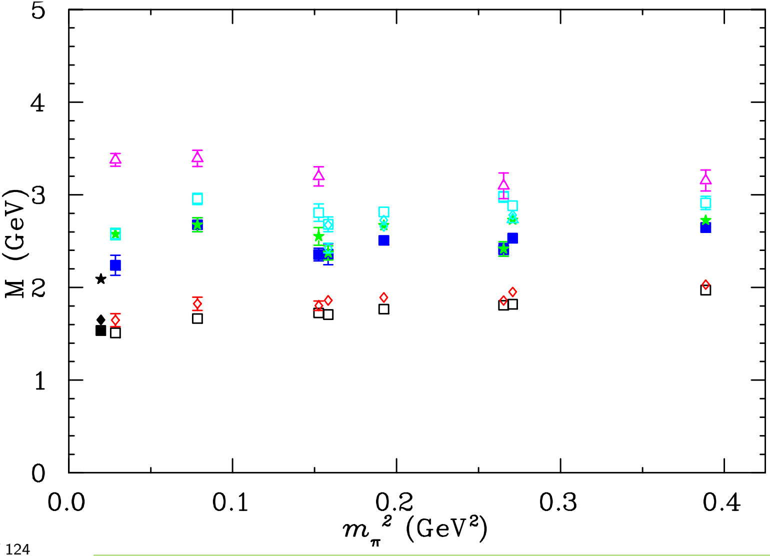

Positive Parity Nucleon Spectrum: χQCD (U. Kentucky) Collaboration

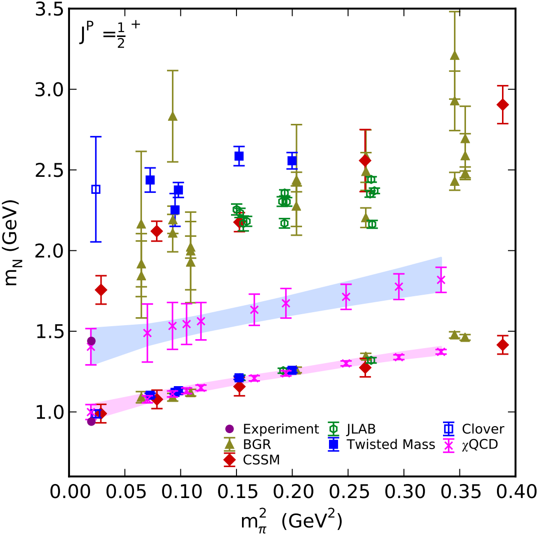

Positive Parity Nucleon Spectrum: χQCD (U. Kentucky) Collaboration

- "The Roper Puzzle,"
  K. F. Liu, Y. Chen, M. Gong, R. Sufian, M. Sun and A. Li,
  PoS LATTICE **2013** (2014) 507
  arXiv:1403.6847 [hep-ph].

- "The Roper Puzzle,"
  K. F. Liu, Y. Chen, M. Gong, R. Sufian, M. Sun and A. Li,
  PoS LATTICE **2013** (2014) 507
  arXiv:1403.6847 [hep-ph].

- Ying Chen's talk in Tuesday's Parallel-B 26-2 at 16:30.

Essence of the Sequential Empirical Bayesian (SEB) Analysis

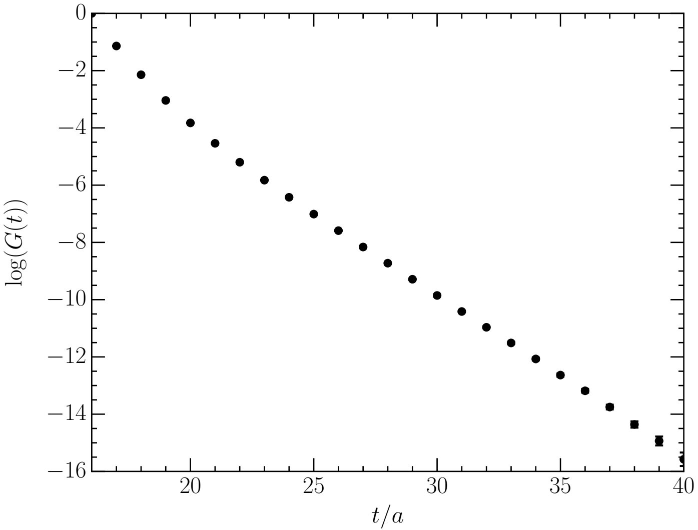

Essence of the Sequential Empirical Bayesian (SEB) Analysis

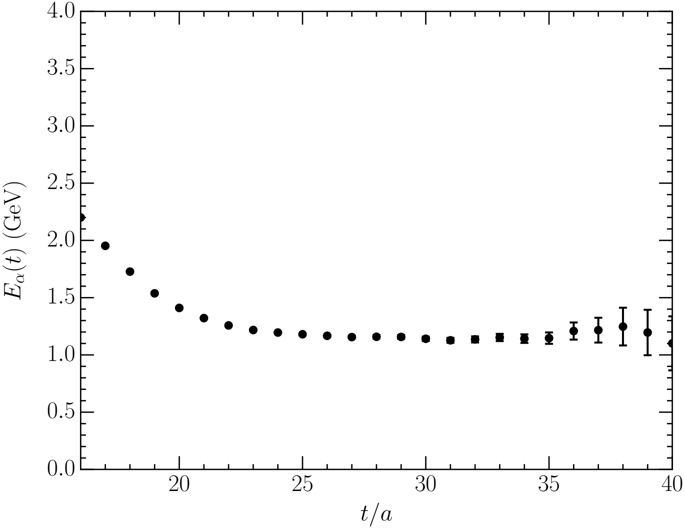

χQCD & HSC Systematic Comparison - Same Correlators Examined

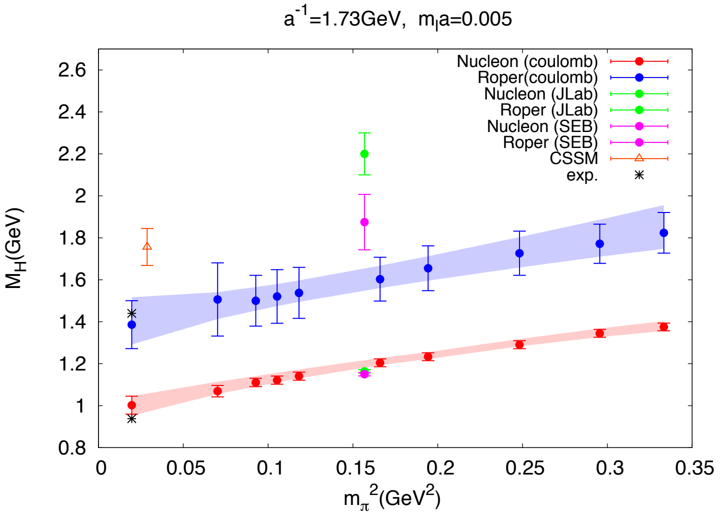

Positive Parity Spectrum: Cypress (Twisted Mass) Collaboration: Feb. '13

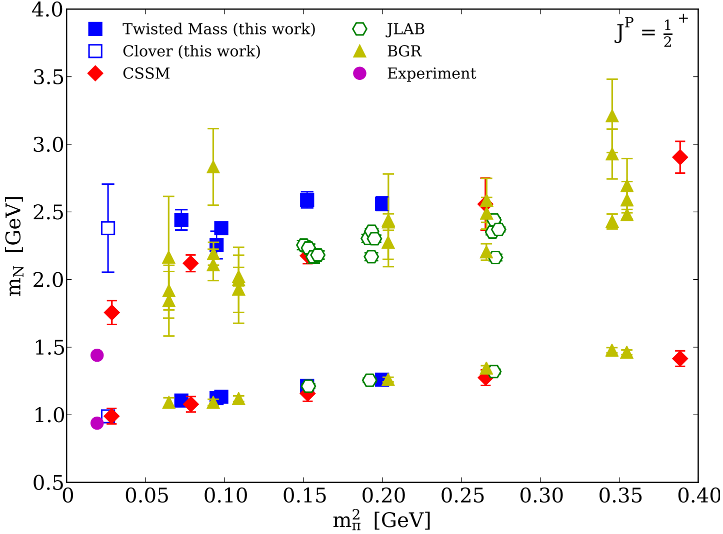

Positive Parity Spectrum: Cypress (Twisted Mass) Collaboration: Jan. '14

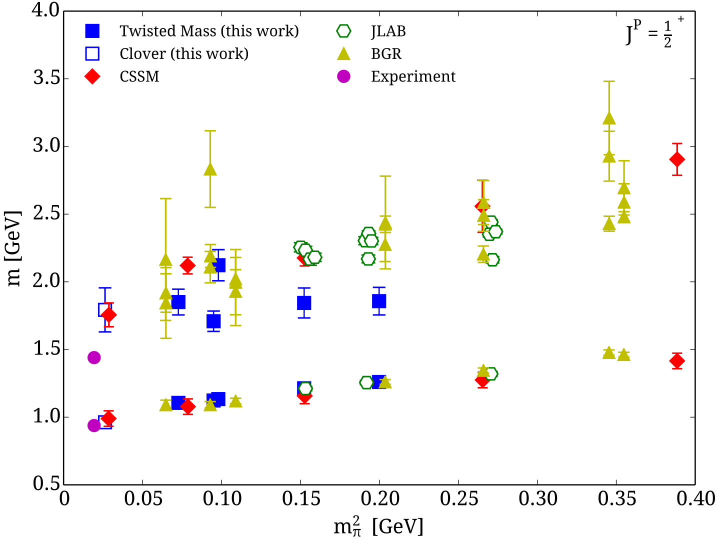

d-quark probability density in ground state proton: $m_\pi = 156$ MeV (CSSM)

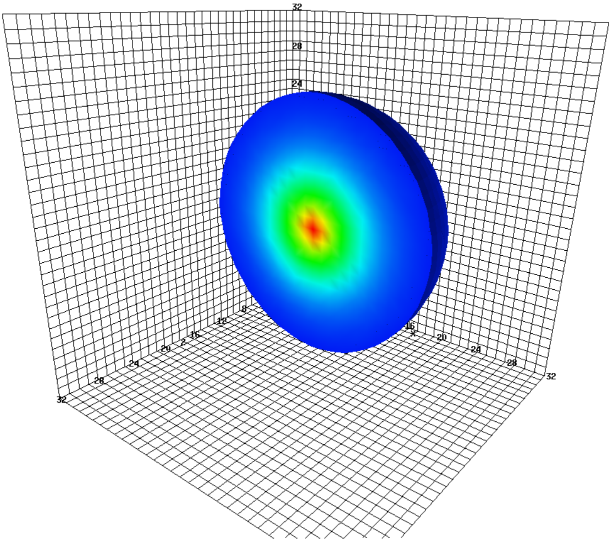

d-quark probability density in first excited proton: $m_\pi = 156$ MeV (CSSM)

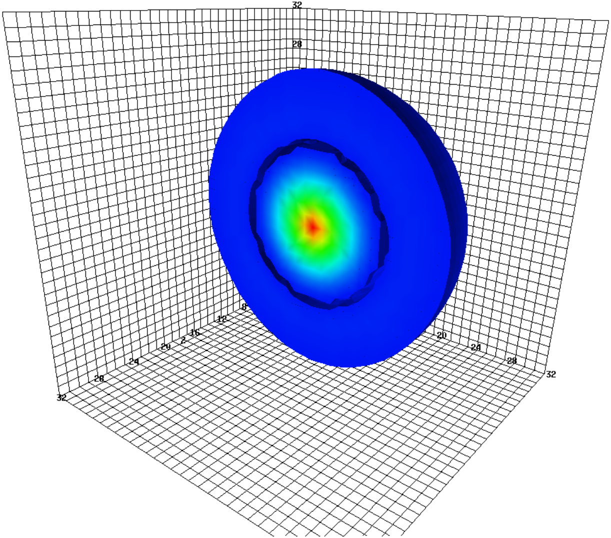

Positive Parity Nucleon Spectrum: only small smearing: Cypress

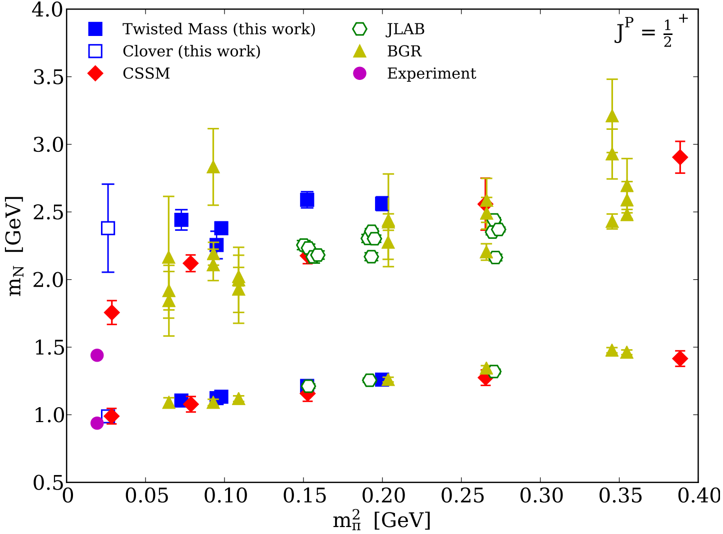

Positive Parity Nucleon Spectrum: r_{RMS} smearing of 8.6 lu: Cypress

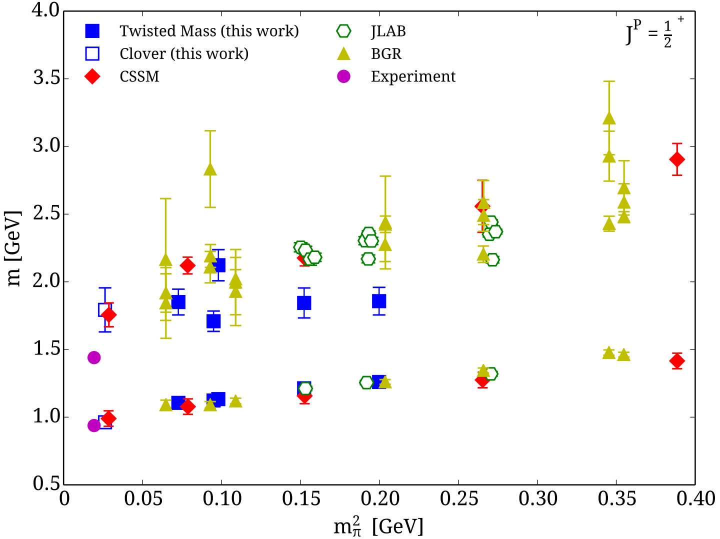

Athens Model Independent Analysis Scheme (AMIAS)

- "Novel analysis method for excited states in lattice QCD: The nucleon case," C. Alexandrou, T. Leontiou, C. N. Papanicolas and E. Stiliaris, Phys. Rev. D **91** (2015) 1, 014506 arXiv:1411.6765 [hep-lat].

Athens Model Independent Analysis Scheme (AMIAS)

- Does not rely on plateau identification of effective masses

Athens Model Independent Analysis Scheme (AMIAS)

- Does not rely on plateau identification of effective masses
- Exploits small time separations where the excited states contribute and statistical errors are small.

Athens Model Independent Analysis Scheme (AMIAS)

- Does not rely on plateau identification of effective masses
- Exploits small time separations where the excited states contribute and statistical errors are small.
- The Correlation matrix has the spectral decomposition

$$G_{ij}(t) = \sum_{\alpha=0}^{N_{\rm states}} A_i^{\alpha} \, A_j^{\dagger\alpha} \, e^{-E_\alpha \, t} \, . \quad i,j = 1, \ldots, N_{\rm interpolators} \, .$$

Athens Model Independent Analysis Scheme (AMIAS)

- Does not rely on plateau identification of effective masses
- Exploits small time separations where the excited states contribute and statistical errors are small.
- The Correlation matrix has the spectral decomposition

$$G_{ij}(t) = \sum_{\alpha=0}^{N_{\mathrm{states}}} A_i^{\alpha} A_j^{\dagger\alpha} e^{-E_\alpha t} . \quad i,j = 1,\ldots,N_{\mathrm{interpolators}} .$$

- Importance sampling is used to select fit parameters, A_i^α and E_α, with the probability $\exp(-\chi^2/2)$.

Athens Model Independent Analysis Scheme (AMIAS)

- Does not rely on plateau identification of effective masses
- Exploits small time separations where the excited states contribute and statistical errors are small.
- The Correlation matrix has the spectral decomposition

$$G_{ij}(t) = \sum_{\alpha=0}^{N_{\mathrm{states}}} A_i^{\alpha} \, A_j^{\dagger\alpha} \, e^{-E_\alpha \, t} \, . \quad i,j = 1,\ldots,N_{\mathrm{interpolators}} \, .$$

- Importance sampling is used to select fit parameters, A_i^{α} and E_α, with the probability $\exp(-\chi^2/2)$.
  - A parallel tempering algorithm is used to avoid local minima traps.

Athens Model Independent Analysis Scheme (AMIAS)

- Does not rely on plateau identification of effective masses
- Exploits small time separations where the excited states contribute and statistical errors are small.
- The Correlation matrix has the spectral decomposition

$$G_{ij}(t) = \sum_{\alpha=0}^{N_{\mathrm{states}}} A_i^{\alpha} A_j^{\dagger\alpha} e^{-E_\alpha t} . \quad i,j = 1, \ldots, N_{\mathrm{interpolators}} .$$

- Importance sampling is used to select fit parameters, A_i^α and E_α, with the probability $\exp(-\chi^2/2)$.
  - A parallel tempering algorithm is used to avoid local minima traps.
- Parameters are determined by fitting a Gaussian to their probability distributions.

Athens Model Independent Analysis Scheme (AMIAS)

- Does not rely on plateau identification of effective masses
- Exploits small time separations where the excited states contribute and statistical errors are small.
- The Correlation matrix has the spectral decomposition

$$G_{ij}(t) = \sum_{\alpha=0}^{N_{\mathrm{states}}} A_i^{\alpha} \, A_j^{\dagger\alpha} \, e^{-E_\alpha \, t} \, . \quad i, j = 1, \ldots, N_{\mathrm{interpolators}} \, .$$

- Importance sampling is used to select fit parameters, A_i^{α} and E_α, with the probability $\exp(-\chi^2/2)$.
    - A parallel tempering algorithm is used to avoid local minima traps.
- Parameters are determined by fitting a Gaussian to their probability distributions.
- Increase N_{states} until there is no sensitivity to additional exponentials.

Determining $N_{\mathrm{states}} \equiv \mathrm{n}_{\mathrm{max}}$ (Cypress)

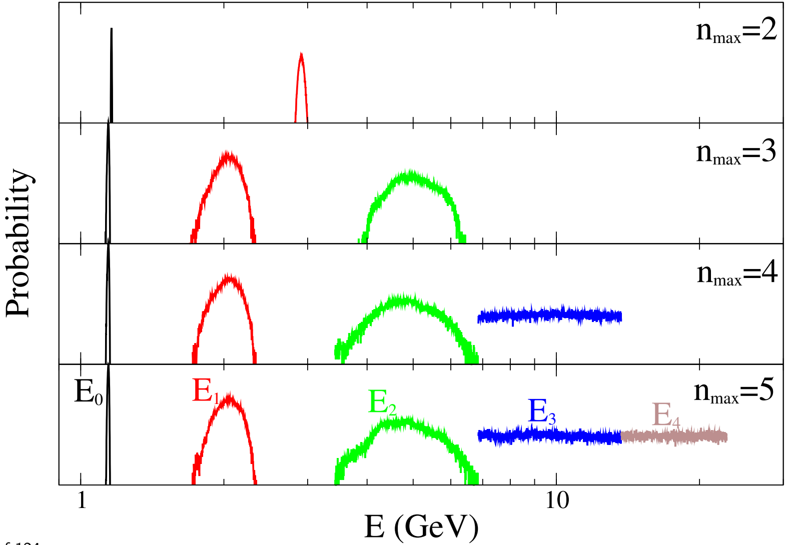

Analysis of Correlation Matrix is Essential

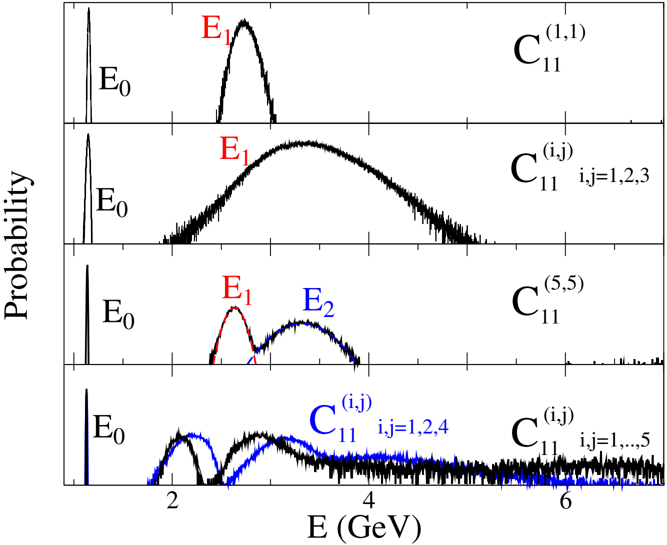

AMIAS applied to positive-parity Cypress results

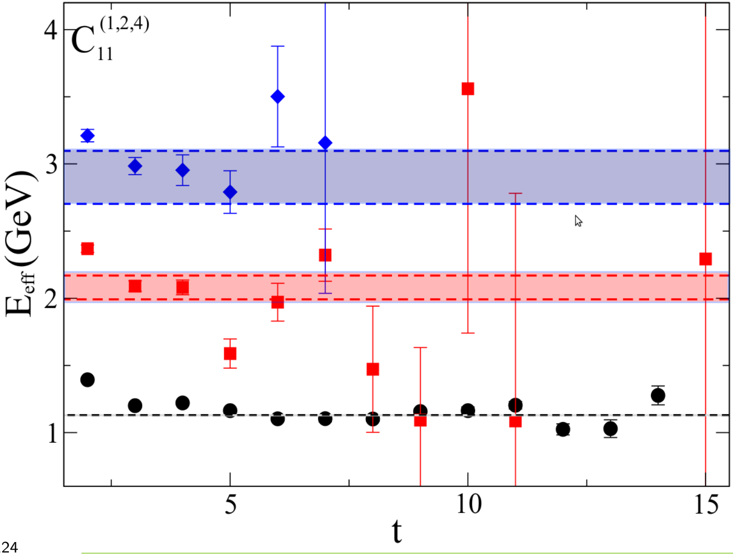

Lowest-lying positive-parity N^* Spectrum

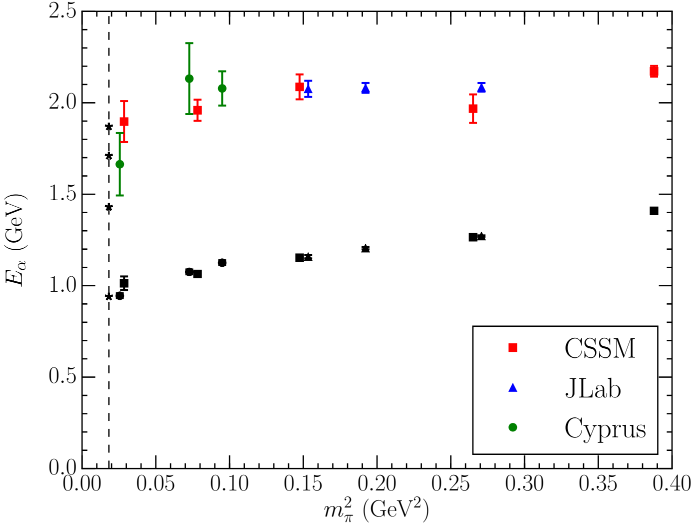

Properties of the Positive Parity Nucleon Spectrum

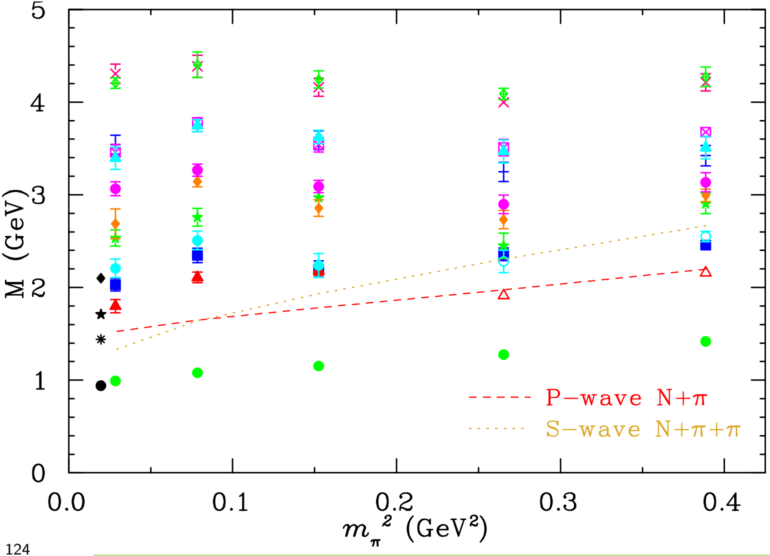

d-quark probability density in ground state proton (CSSM)

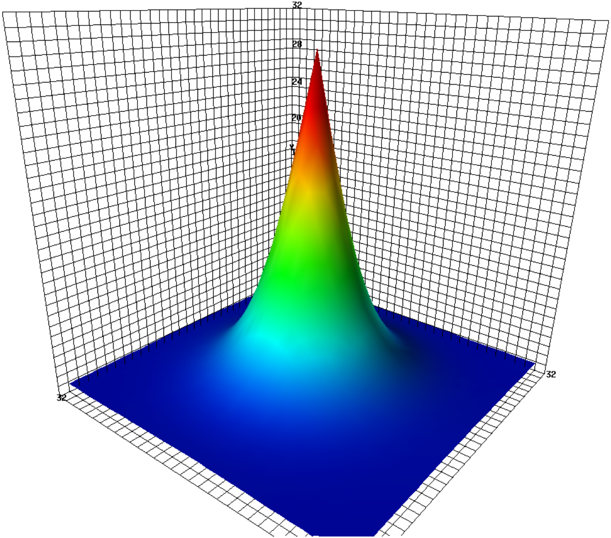

d-quark probability density in 1st excited state of proton (CSSM)

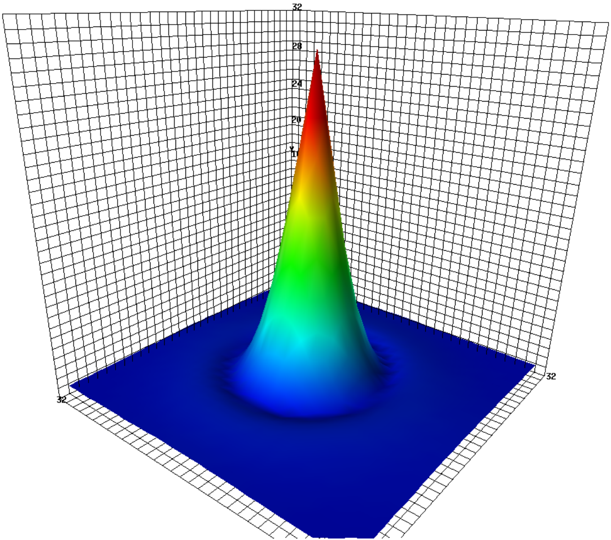

d-quark probability density in $N = 3$ excited state of proton (CSSM)

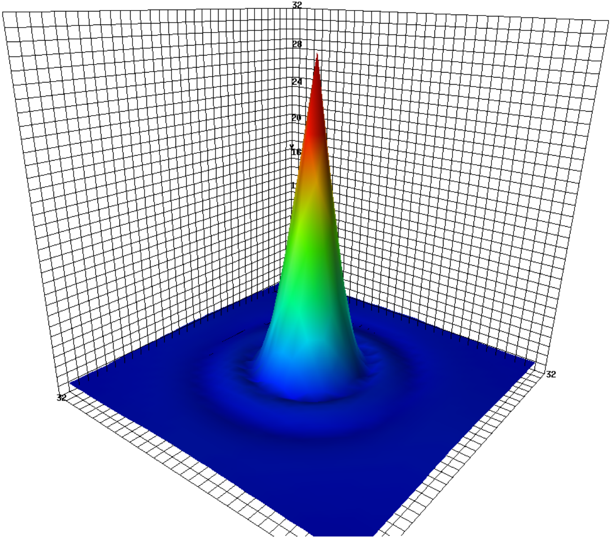

d-quark probability density in $N = 4$ excited state of proton (CSSM)

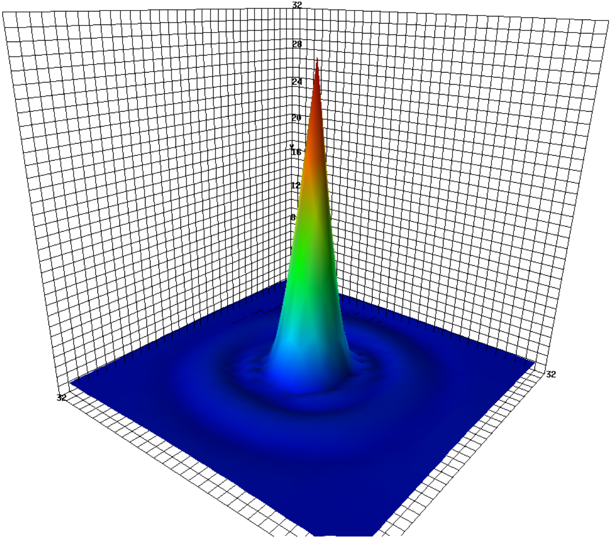

Comparison with the Simple Quark Model - CSSM

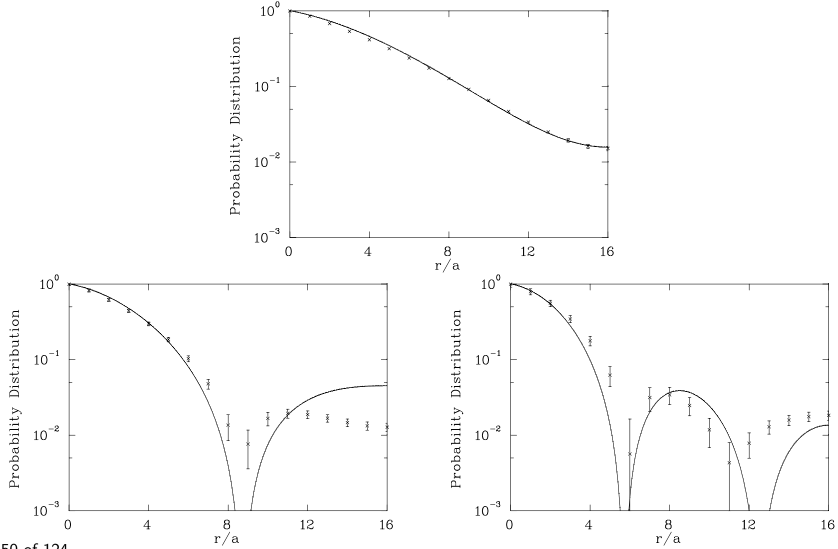

d-quark probability density in 1st excited state of proton (CSSM)

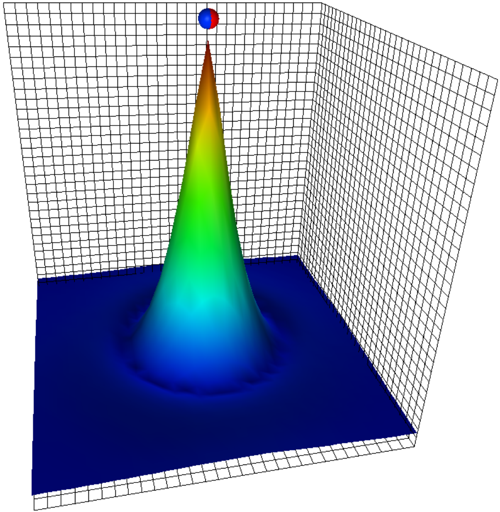

d-quark probability density in 1st excited state of proton (CSSM)

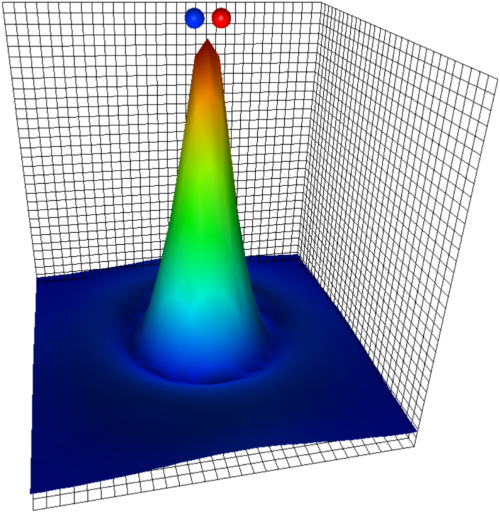

d-quark probability density in 1st excited state of proton (CSSM)

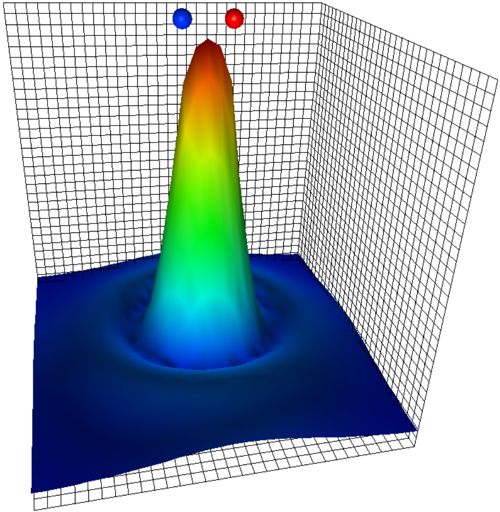

d-quark probability density in 1st excited state of proton (CSSM)

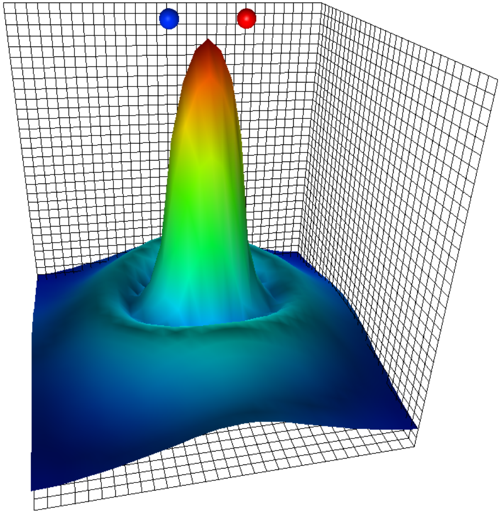

d-quark probability density in 1st excited state of proton (CSSM)

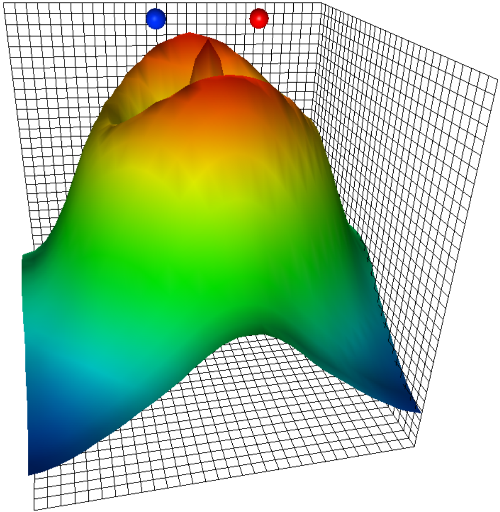

d-quark probability density in 1st excited state of proton (CSSM)

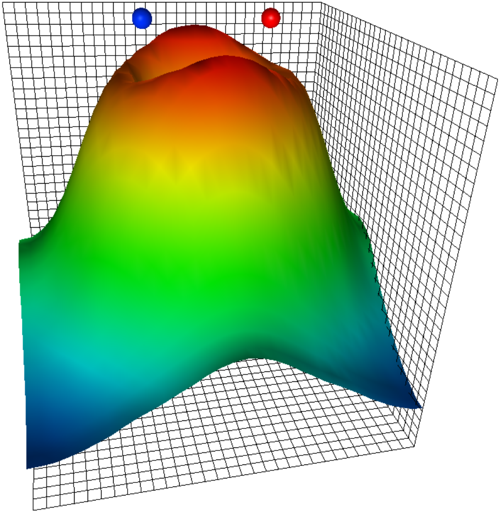

d-quark probability density in 1st excited state of proton (CSSM)

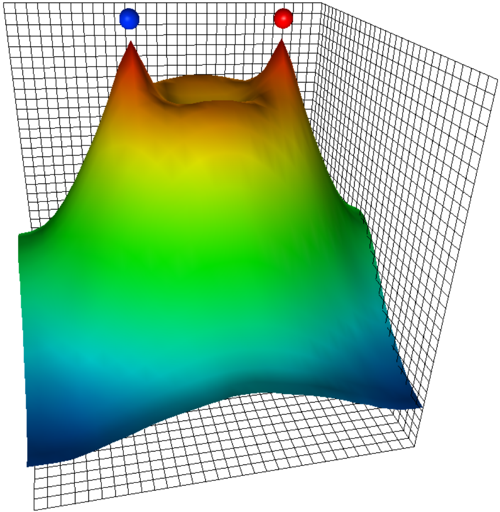

d-quark probability density in 1st excited state of proton (CSSM)

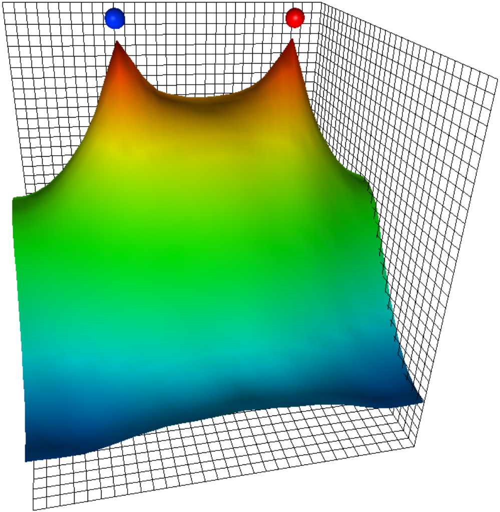

d-quark probability density in 4th excited state of proton (CSSM)

PHYSICAL REVIEW D

particles, fields, gravitation, and cosmology

Highlights Recent Accepted Authors Referees Search About

Kaleidoscope

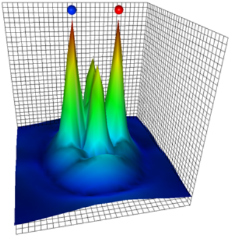

From the article:

Nucleon excited state wave functions from lattice QCD

Dale S. Roberts, Waseem Kamleh, and Derek B. Leinweber

Phys. Rev. D **89**, 074501 (2014)

Form Factors of positive-parity nucleon excitations

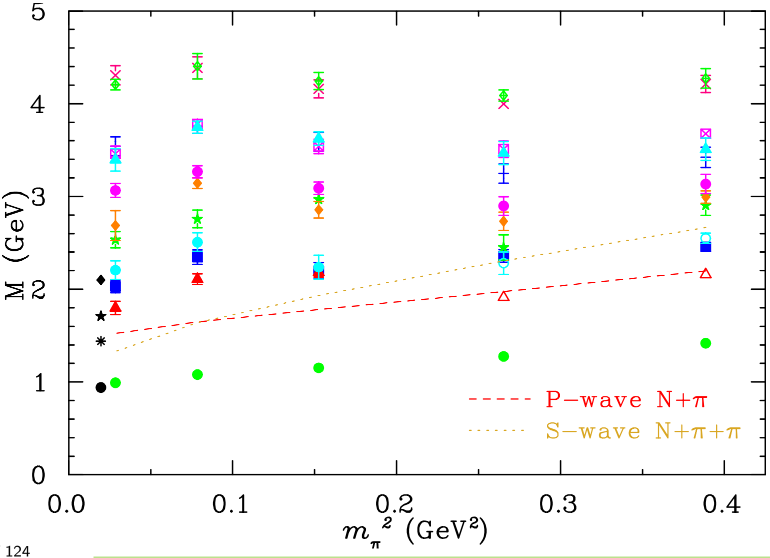

Charge Radii of the Proton, Delta and “Roper”

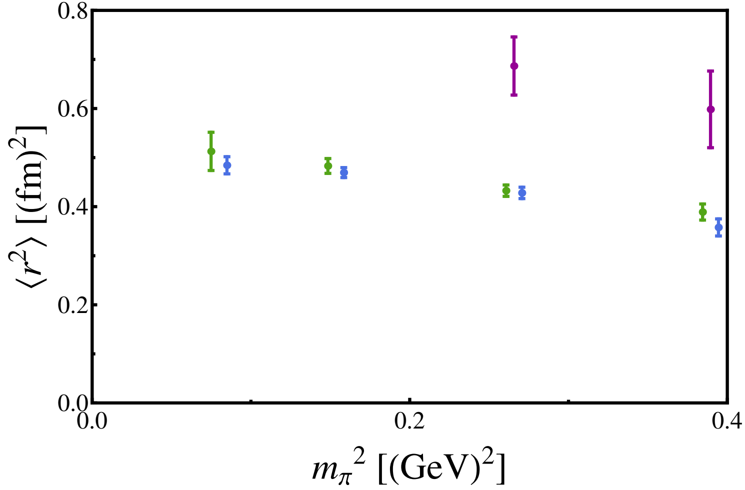

Magnetic Moments of the Proton, Delta and "Roper"

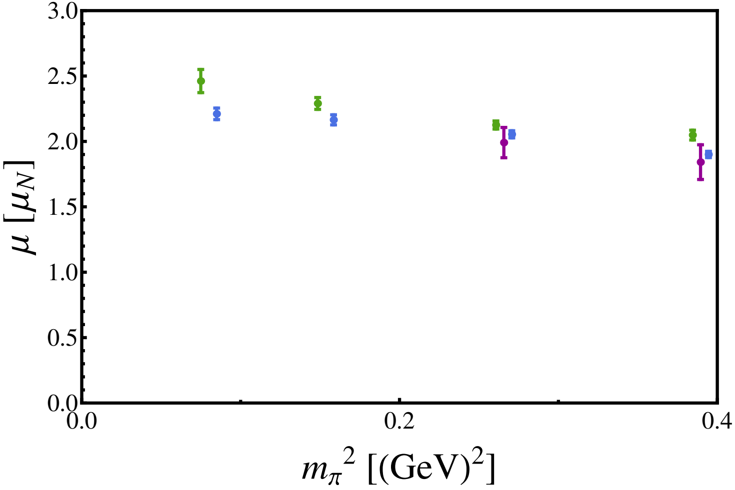

Magnetic Moments of the odd-parity p^*, and n^*

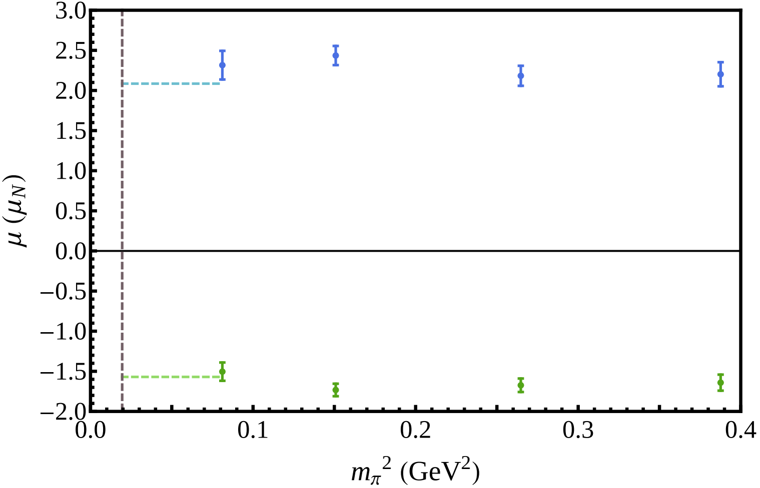

- Comparison with quark model result of N. Sharma, *et al.* (2013).

References

- "Nucleon Excited State Wave Functions from Lattice QCD,"
  D. S. Roberts, W. Kamleh and D. B. Leinweber.
  Phys. Rev. **D89** (2014) 074501 arXiv:1311.6626 [hep-lat]

- "Electromagnetic matrix elements for negative parity nucleons,"
  B. Owen, W. Kamleh, D. Leinweber, S. Mahbub and B. Menadue
  PoS LATTICE **2014** (2014) 159 arXiv:1412.4432 [hep-lat]

- "Probing the proton and its excitations in full QCD,"
  B. J. Owen, W. Kamleh, D. B. Leinweber, M. S. Mahbub and
  B. J. Menadue
  PoS LATTICE **2013** (2013) 277 arXiv:1312.0291 [hep-lat]

References

- "Nucleon Excited State Wave Functions from Lattice QCD," D. S. Roberts, W. Kamleh and D. B. Leinweber. Phys. Rev. **D89** (2014) 074501 arXiv:1311.6626 [hep-lat]

- "Electromagnetic matrix elements for negative parity nucleons," B. Owen, W. Kamleh, D. Leinweber, S. Mahbub and B. Menadue PoS LATTICE **2014** (2014) 159 arXiv:1412.4432 [hep-lat]

- "Probing the proton and its excitations in full QCD," B. J. Owen, W. Kamleh, D. B. Leinweber, M. S. Mahbub and B. J. Menadue PoS LATTICE **2013** (2013) 277 arXiv:1312.0291 [hep-lat]

- "Magnetic moments of the low-lying $1/2^-$ octet baryon resonances," N. Sharma, A. Martinez Torres, K. P. Khemchandani and H. Dahiya Eur. Phys. J. A **49** (2013) 11 [arXiv:1207.3311 [hep-ph]]

Have we seen the Roper?

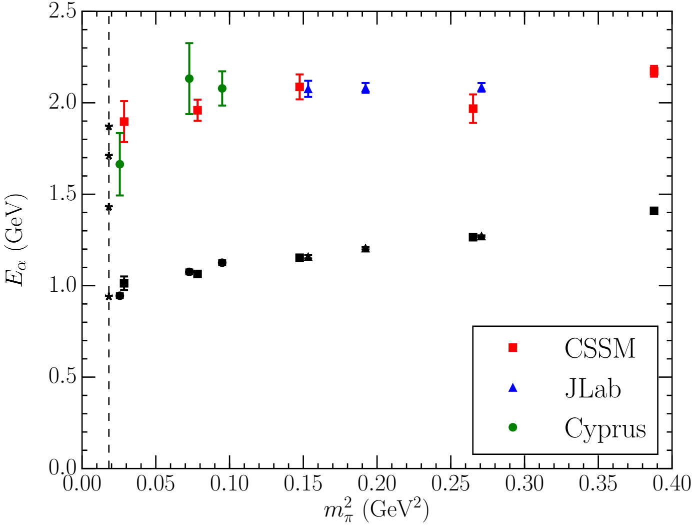

Finite-Volume Effect in $N = 2$ excited state: $m_\pi = 702$ MeV

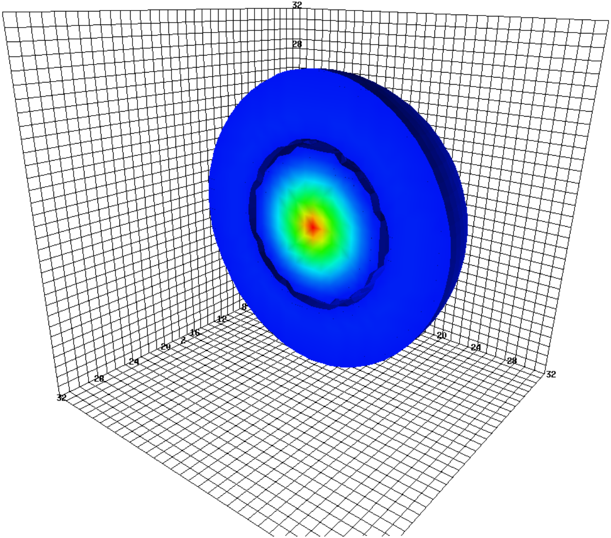

Finite-Volume Effect in $N = 2$ excited state: $m_\pi = 570$ MeV

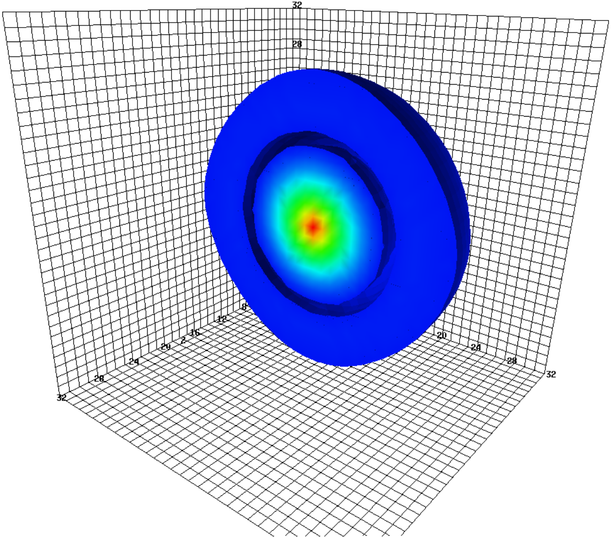

Finite-Volume Effect in $N = 2$ excited state: $m_\pi = 411$ MeV

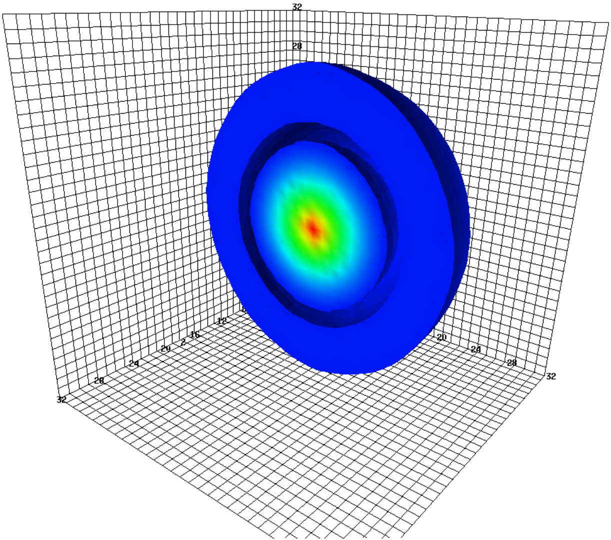

Finite-Volume Effect in $N = 2$ excited state: $m_\pi = 296$ MeV

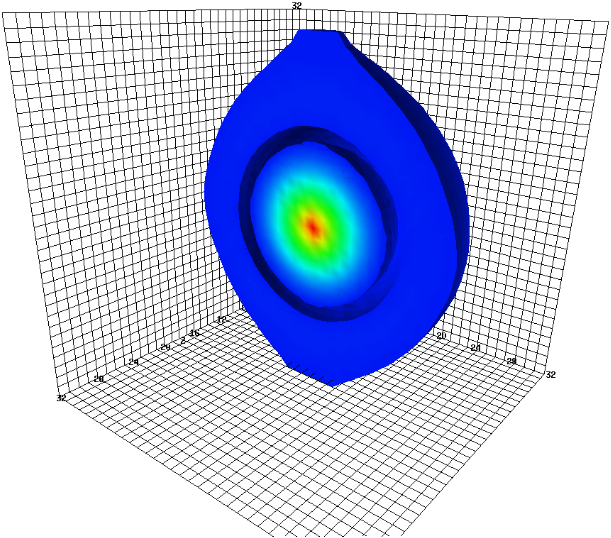

Finite-Volume Effect in $N = 2$ excited state: $m_\pi = 156$ MeV

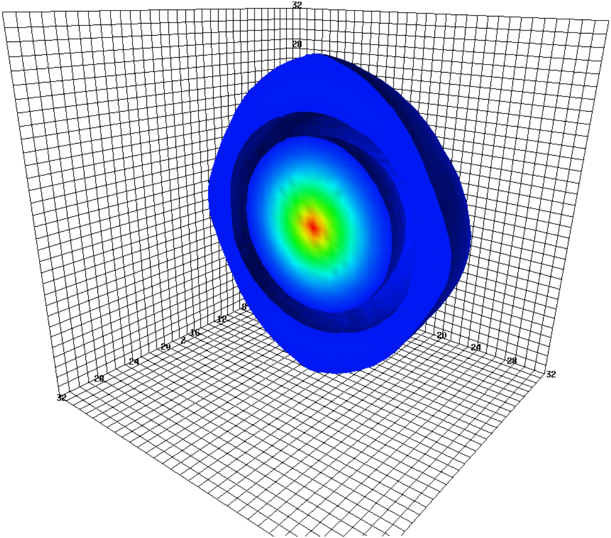

Have we seen the Roper?

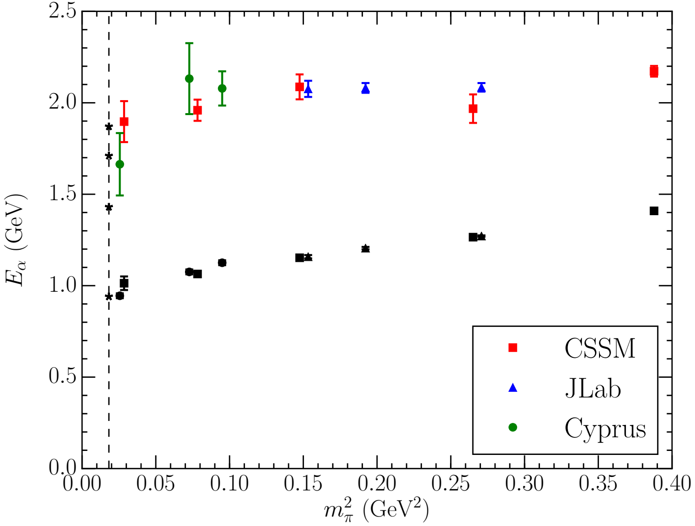

Hamiltonian Effective Field Theory

- Zhan-Wei Liu, Jiajun Wu, *et al.* [CSSM]
  In preparation.

Hamiltonian Effective Field Theory

- Zhan-Wei Liu, Jiajun Wu, *et al.* [CSSM]
  In preparation.

- Jiajun Wu's talk in Wednesday's Parallel-B 27-1 at 15:30.

Hamiltonian Effective Field Theory

- Zhan-Wei Liu, Jiajun Wu, *et al.* [CSSM]
  In preparation.

- Jiajun Wu's talk in Wednesday's Parallel-B 27-1 at 15:30.

- J. M. M. Hall, *et al.* [CSSM]
  "Lattice QCD Evidence that the $\Lambda(1405)$ Resonance is an Antikaon-Nucleon Molecule"
  Phys. Rev. Lett. **114**, 132002 (2015). arXiv:1411.3402 [hep-lat]

- "On the Structure of the $\Lambda(1405)$",
  J. M. M. Hall, *et al.* [CSSM]
  PoS LATTICE **2014**, 094 (2014). arXiv:1411.3781 [hep-lat]

Hamiltonian Effective Field Theory Model

- Consider the $\Lambda(1405)$.

Hamiltonian Effective Field Theory Model

- Consider the $\Lambda(1405)$.
- The four octet meson-baryon interaction channels of the $\Lambda(1405)$ are considered: $\pi\Sigma$, $\overline{K}N$, $K\Xi$ and $\eta\Lambda$.

Hamiltonian Effective Field Theory Model

- Consider the $\Lambda(1405)$.
- The four octet meson-baryon interaction channels of the $\Lambda(1405)$ are considered: $\pi\Sigma$, $\overline{K}N$, $K\Xi$ and $\eta\Lambda$.
- A single-particle state with bare mass, $m_0 + \alpha_0\, m_\pi^2$ is also included.

Hamiltonian Effective Field Theory Model

- Consider the $\Lambda(1405)$.
- The four octet meson-baryon interaction channels of the $\Lambda(1405)$ are considered: $\pi\Sigma$, $\overline{K}N$, $K\Xi$ and $\eta\Lambda$.
- A single-particle state with bare mass, $m_0 + \alpha_0\, m_\pi^2$ is also included.
- In a finite periodic volume, momentum is quantised to $n\,(2\pi/L)$.

Hamiltonian Effective Field Theory Model

- Consider the $\Lambda(1405)$.
- The four octet meson-baryon interaction channels of the $\Lambda(1405)$ are considered: $\pi\Sigma$, $\overline{K}N$, $K\Xi$ and $\eta\Lambda$.
- A single-particle state with bare mass, $m_0 + \alpha_0\, m_\pi^2$ is also included.
- In a finite periodic volume, momentum is quantised to $n\,(2\pi/L)$.
- Working on a cubic volume of extent L on each side, it is convenient to define the momentum magnitudes

$$k_n = \sqrt{n_x^2 + n_y^2 + n_z^2}\,\frac{2\pi}{L}\,,$$

with $n_i = 0, 1, 2, \ldots$ and integer $n = n_x^2 + n_y^2 + n_z^2$.

Hamiltonian model, H_0

Denoting each meson-baryon energy by $\omega_{MB}(k_n) = \omega_M(k_n) + \omega_B(k_n)$, with $\omega_A(k_n) \equiv \sqrt{k_n^2 + m_A^2}$, the non-interacting Hamiltonian takes the form

$$H_0 = \begin{pmatrix} m_0 + \alpha_0\, m_\pi^2 & 0 & 0 & \cdots \\ 0 & \begin{matrix}\omega_{\pi\Sigma}(k_0) & \\ & \omega_{\eta\Lambda}(k_0)\end{matrix} & 0 & \cdots \\ 0 & 0 & \begin{matrix}\omega_{\pi\Sigma}(k_1) & \\ & \omega_{\eta\Lambda}(k_1)\end{matrix} & \cdots \\ \vdots & \vdots & \vdots & \ddots \end{pmatrix}.$$

Hamiltonian model, H_I

- Interaction entries describe the coupling of the single-particle state to the two-particle meson-baryon states.

Hamiltonian model, H_I

- Interaction entries describe the coupling of the single-particle state to the two-particle meson-baryon states.
- Each entry represents the S-wave interaction energy of the $\Lambda(1405)$ with one of the four channels at a certain value for k_n.

$$H_I = \begin{pmatrix} 0 & g_{\pi\Sigma}(k_0) & \cdots & g_{\eta\Lambda}(k_0) & g_{\pi\Sigma}(k_1) & \cdots & g_{\eta\Lambda}(k_1)\cdots \\ g_{\pi\Sigma}(k_0) & 0 & \cdots & & & & \\ \vdots & \vdots & 0 & & & & \\ & & & \ddots & & & \\ g_{\eta\Lambda}(k_0) & & & & & & \\ g_{\pi\Sigma}(k_1) & & & & & & \\ \vdots & & & & & & \\ g_{\eta\Lambda}(k_1) & & & & & & \\ \vdots & & & & & & \end{pmatrix} .$$

Eigenvalue Equation Form

- The eigenvalue equation corresponding to our Hamiltonian model is

$$\lambda = m_0 + \alpha_0 \, m_\pi^2 - \sum_{M,B} \sum_{n=0}^{\infty} \frac{g_{MB}^2(k_n)}{\omega_{MB}(k_n) - \lambda} \, .$$

with λ denoting the energy eigenvalue.

Eigenvalue Equation Form

- The eigenvalue equation corresponding to our Hamiltonian model is

$$\lambda = m_0 + \alpha_0 \, m_\pi^2 - \sum_{M,B} \sum_{n=0}^{\infty} \frac{g_{MB}^2(k_n)}{\omega_{MB}(k_n) - \lambda} \, .$$

  with λ denoting the energy eigenvalue.
- As λ is finite, the pole in the denominator of the right-hand side is never accessed.
- The bare mass $m_0 + \alpha_0 \, m_\pi^2$ encounters self-energy corrections that lead to avoided level-crossings in the finite-volume energy eigenstates.

Eigenvalue Equation Form

- The eigenvalue equation corresponding to our Hamiltonian model is

$$\lambda = m_0 + \alpha_0\, m_\pi^2 - \sum_{M,B} \sum_{n=0}^{\infty} \frac{g_{MB}^2(k_n)}{\omega_{MB}(k_n) - \lambda}\,.$$

  with λ denoting the energy eigenvalue.
- As λ is finite, the pole in the denominator of the right-hand side is never accessed.
- The bare mass $m_0 + \alpha_0\, m_\pi^2$ encounters self-energy corrections that lead to avoided level-crossings in the finite-volume energy eigenstates.
- Reference to chiral effective field theory provides the form of $g_{MB}(k_n)$.

Hamiltonian model solution and fit

- The LAPACK software library routine `dgeev` is used to obtain the eigenvalues and eigenvectors of H.

Hamiltonian model solution and fit

- The LAPACK software library routine `dgeev` is used to obtain the eigenvalues and eigenvectors of H.
- The bare mass parameters m_0 and α_0 are determined by a fit to the lattice QCD results.

Hamiltonian model fit

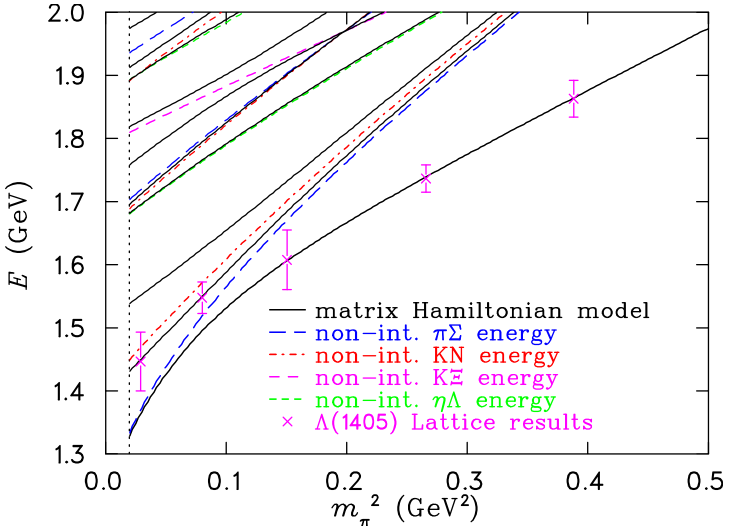

Avoided Level Crossing

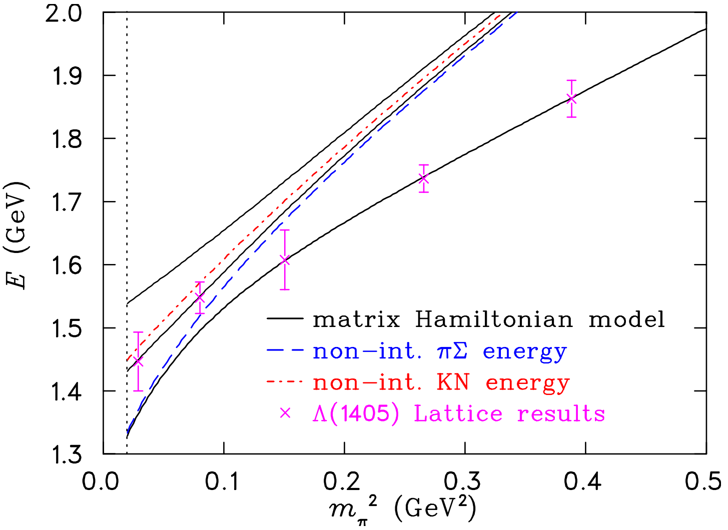

Energy eigenstate, $|E\rangle$, basis $|state\rangle$ composition

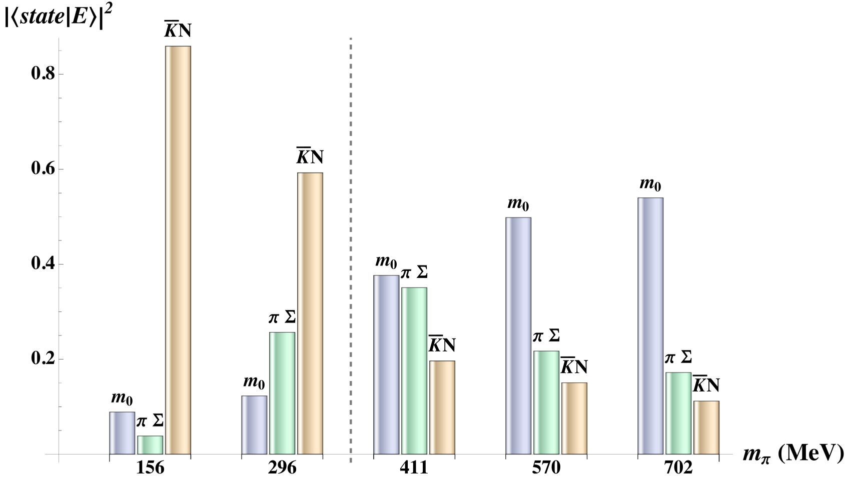

Strange Magnetic Form Factor

- Provides direct insight into the possible dominance of a molecular $\overline{K}N$ bound state.

Strange Magnetic Form Factor

- Provides direct insight into the possible dominance of a molecular $\overline{K}N$ bound state.
- In forming such a molecular state, the $\Lambda(u, d, s)$ valence quark configuration is complemented by
  - A $u, \overline{u}$ pair making a $K^-(s, \overline{u})$ - proton (u, u, d) bound state, or
  - A $d, \overline{d}$ pair making a $\overline{K}^0(s, \overline{d})$ - neutron (d, d, u) bound state.

Strange Magnetic Form Factor

- Provides direct insight into the possible dominance of a molecular $\overline{K}N$ bound state.
- In forming such a molecular state, the $\Lambda(u, d, s)$ valence quark configuration is complemented by
  - A $u, \overline{u}$ pair making a $K^-(s, \overline{u})$ - proton (u, u, d) bound state, or
  - A $d, \overline{d}$ pair making a $\overline{K}^0(s, \overline{d})$ - neutron (d, d, u) bound state.
- In both cases the strange quark is confined within a spin-0 kaon and has no preferred spin orientation.

Strange Magnetic Form Factor

- Provides direct insight into the possible dominance of a molecular $\overline{K}N$ bound state.
- In forming such a molecular state, the $\Lambda(u, d, s)$ valence quark configuration is complemented by
  - A $u, \overline{u}$ pair making a $K^-(s, \overline{u})$ - proton (u, u, d) bound state, or
  - A $d, \overline{d}$ pair making a $\overline{K}^0(s, \overline{d})$ - neutron (d, d, u) bound state.
- In both cases the strange quark is confined within a spin-0 kaon and has no preferred spin orientation.
- To conserve parity, the kaon has zero orbital angular momentum.

Strange Magnetic Form Factor

- Provides direct insight into the possible dominance of a molecular $\overline{K}N$ bound state.
- In forming such a molecular state, the $\Lambda(u, d, s)$ valence quark configuration is complemented by
  - A $u, \overline{u}$ pair making a $K^-(s, \overline{u})$ - proton (u, u, d) bound state, or
  - A $d, \overline{d}$ pair making a $\overline{K}^0(s, \overline{d})$ - neutron (d, d, u) bound state.
- In both cases the strange quark is confined within a spin-0 kaon and has no preferred spin orientation.
- To conserve parity, the kaon has zero orbital angular momentum.
- Thus, the strange quark does not contribute to the magnetic form factor of the $\Lambda(1405)$ when it is in a $\overline{K}N$ molecule.

$\mathcal{G}_M$ for the $\Lambda(1405)$ at $Q^2 \sim 0.16\,\mathrm{GeV}^2$

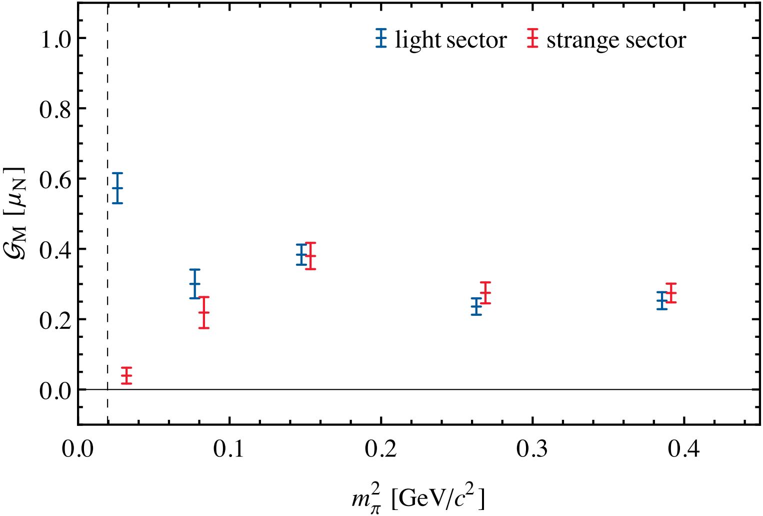

Low-lying odd-parity nucleon (N^*) states

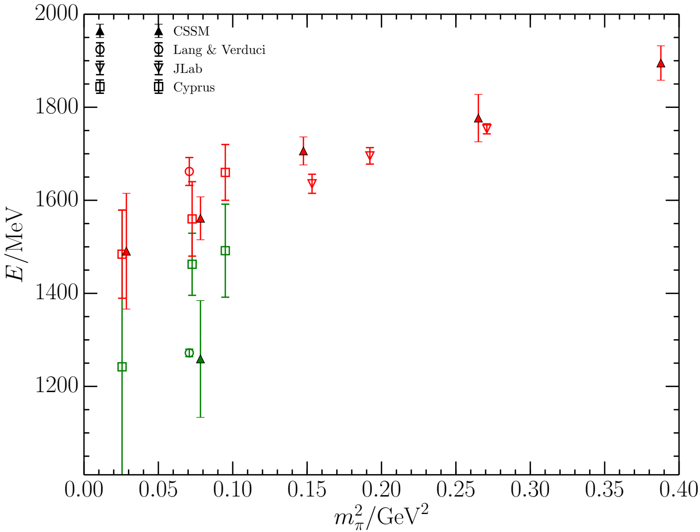

Non-interacting meson-baryon channels considered

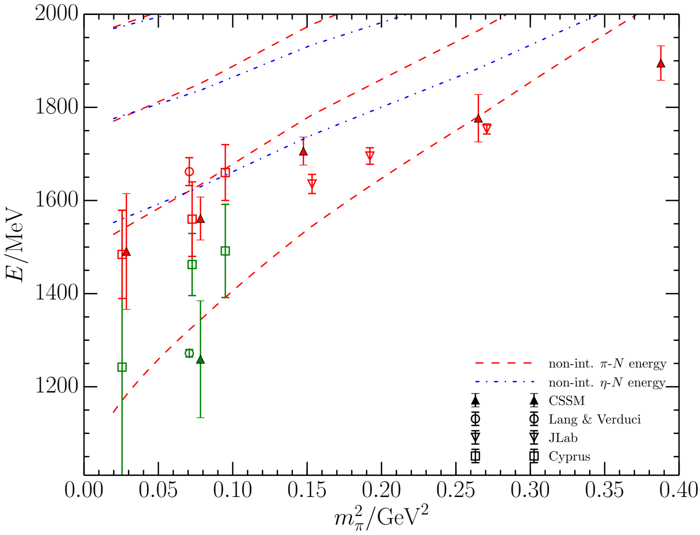

Hamiltonian Model N^* Spectrum: 3 fm

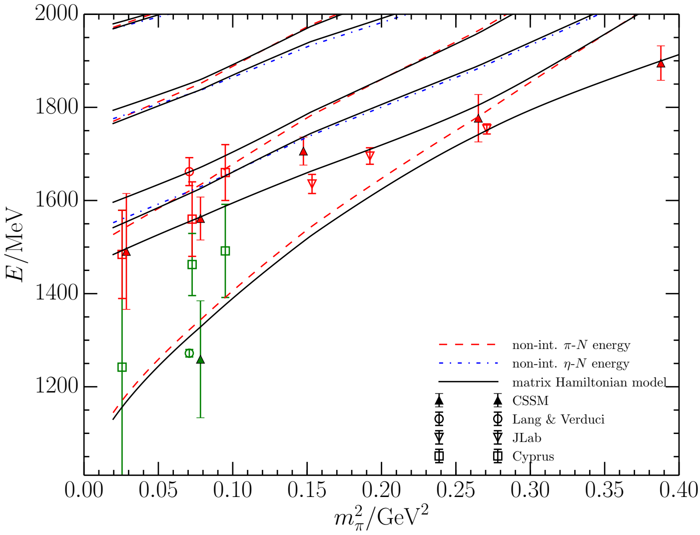

Hamiltonian Model N^* Spectrum: 3 fm

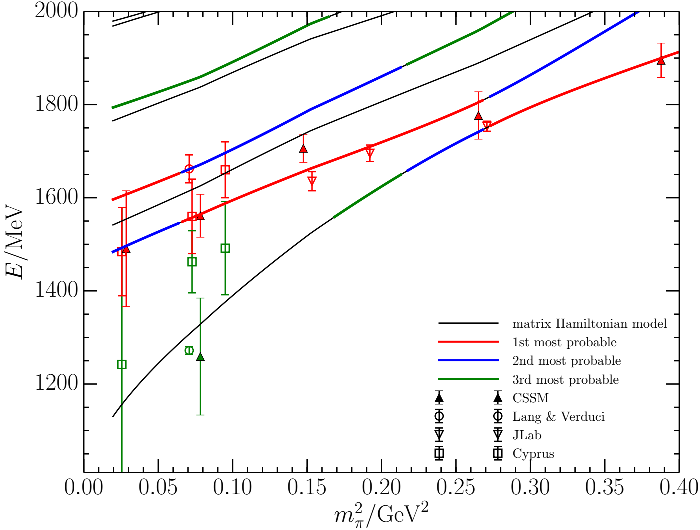

Hamiltonian Model N^* Spectrum: 2 fm

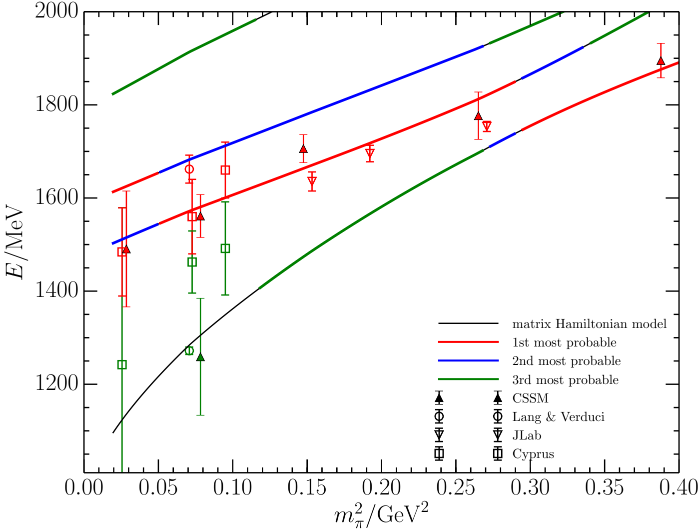

Volume Dependence of the N^* Spectrum

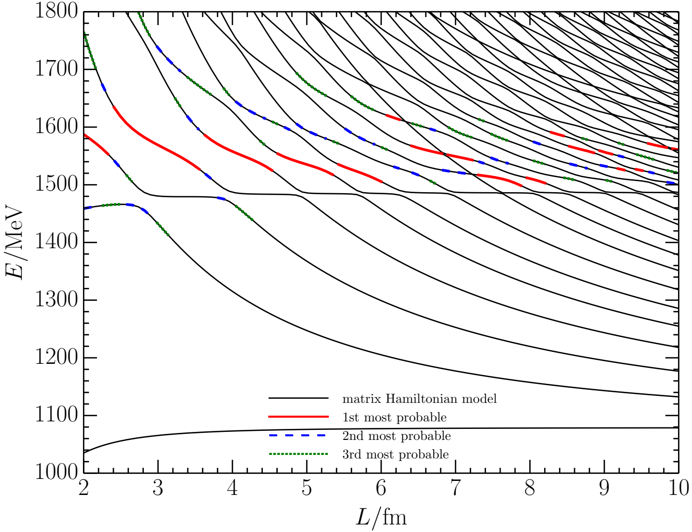

Hamiltonian Model N^* Spectrum: 3 fm

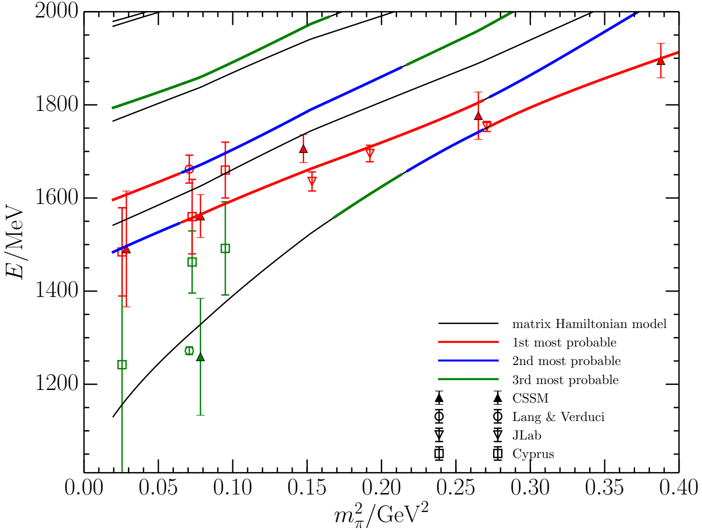

What about the Roper?

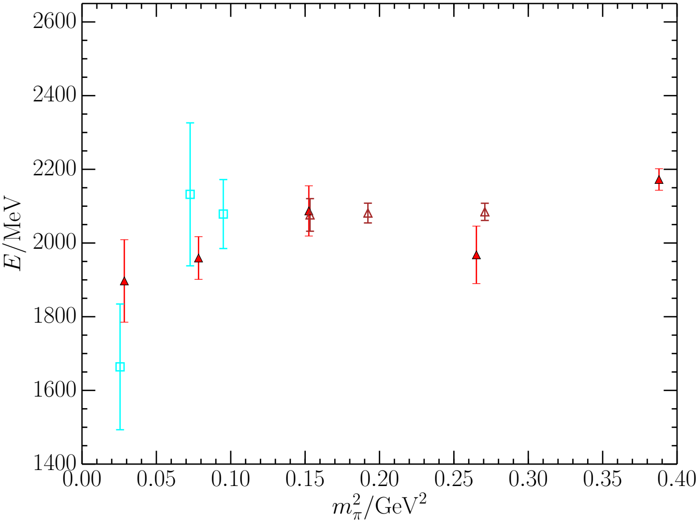

Non-interacting meson-baryon channels considered

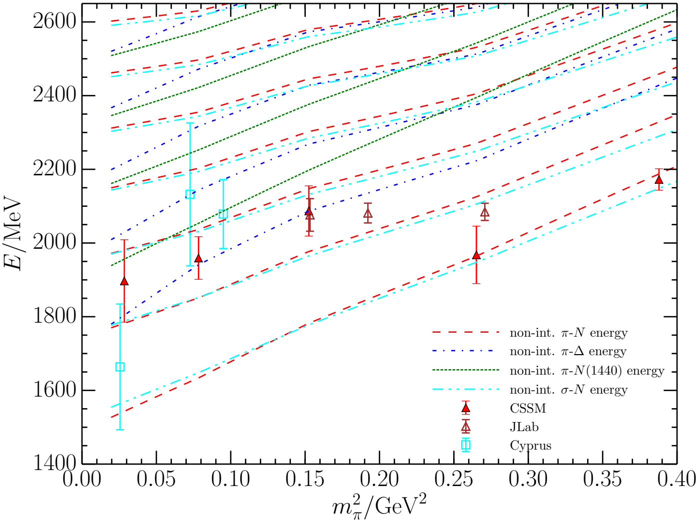

Hamiltonian Model N' Spectrum

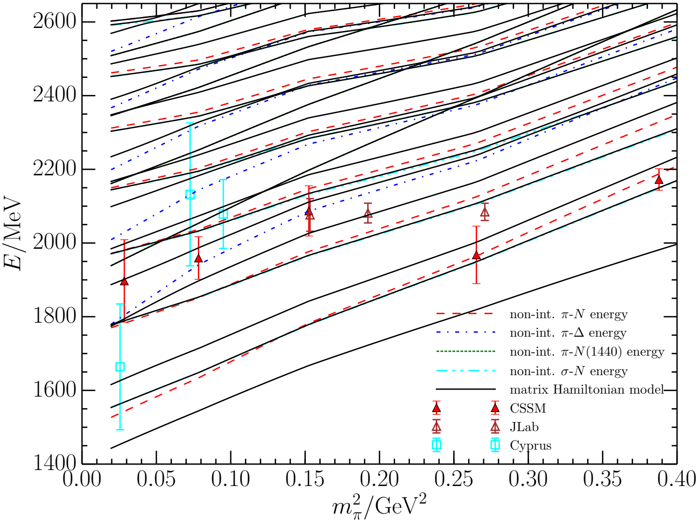

Hamiltonian Model N' Spectrum

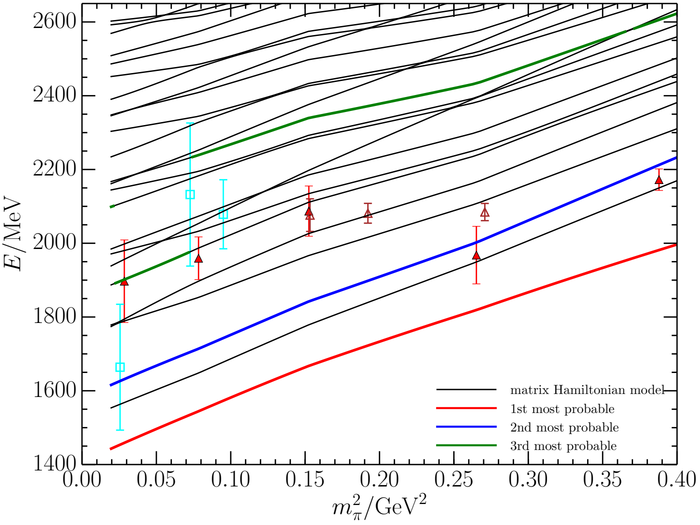

Hamiltonian N' Spectrum: Increased bare mass slope

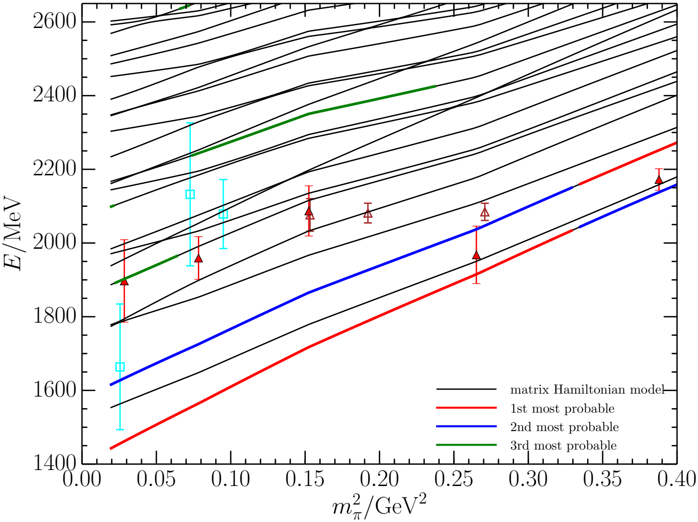

Bare State Strength in the N' Spectrum: 3 fm

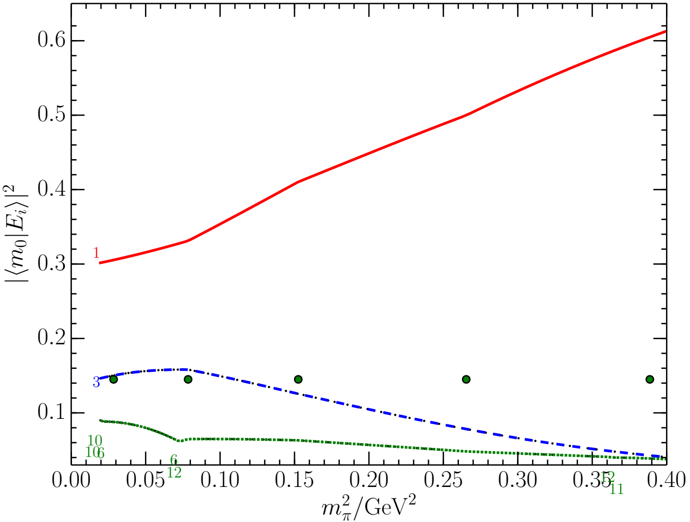

Conclusions

- A survey of the current literature resolves discrepancies among groups exploring the low-lying nucleon spectrum.
  - Results for low-lying nucleon excitations are forming a consensus.

Conclusions

- A survey of the current literature resolves discrepancies among groups exploring the low-lying nucleon spectrum.
  - Results for low-lying nucleon excitations are forming a consensus.
- The negative parity sector appears to be well understood.
  - Hamiltonian Effective Field Theory describes the spectrum well.

Conclusions

- A survey of the current literature resolves discrepancies among groups exploring the low-lying nucleon spectrum.
  - Results for low-lying nucleon excitations are forming a consensus.
- The negative parity sector appears to be well understood.
  - Hamiltonian Effective Field Theory describes the spectrum well.
  - First results for form factors are consistent with model expectations

Conclusions

- A survey of the current literature resolves discrepancies among groups exploring the low-lying nucleon spectrum.
  - Results for low-lying nucleon excitations are forming a consensus.
- The negative parity sector appears to be well understood.
  - Hamiltonian Effective Field Theory describes the spectrum well.
  - First results for form factors are consistent with model expectations
- Roper of the Constituent Quark Model has been seen on the lattice.
  - Node structure and density is similar to model expectations.

Conclusions

- A survey of the current literature resolves discrepancies among groups exploring the low-lying nucleon spectrum.
  - Results for low-lying nucleon excitations are forming a consensus.
- The negative parity sector appears to be well understood.
  - Hamiltonian Effective Field Theory describes the spectrum well.
  - First results for form factors are consistent with model expectations
- Roper of the Constituent Quark Model has been seen on the lattice.
  - Node structure and density is similar to model expectations.
- The structure of the $\Lambda(1405)$ is dominated by a molecular bound state of an anti-kaon and a nucleon.

Conclusions

- A survey of the current literature resolves discrepancies among groups exploring the low-lying nucleon spectrum.
  - Results for low-lying nucleon excitations are forming a consensus.
- The negative parity sector appears to be well understood.
  - Hamiltonian Effective Field Theory describes the spectrum well.
  - First results for form factors are consistent with model expectations
- Roper of the Constituent Quark Model has been seen on the lattice.
  - Node structure and density is similar to model expectations.
- The structure of the $\Lambda(1405)$ is dominated by a molecular bound state of an anti-kaon and a nucleon.
- The Roper of Nature has yet to be seen in the light quark mass regime.

Supplementary Information

The following slides provide additional information which may be of interest.

Bare State Strength in the N^* Spectrum: 3 fm

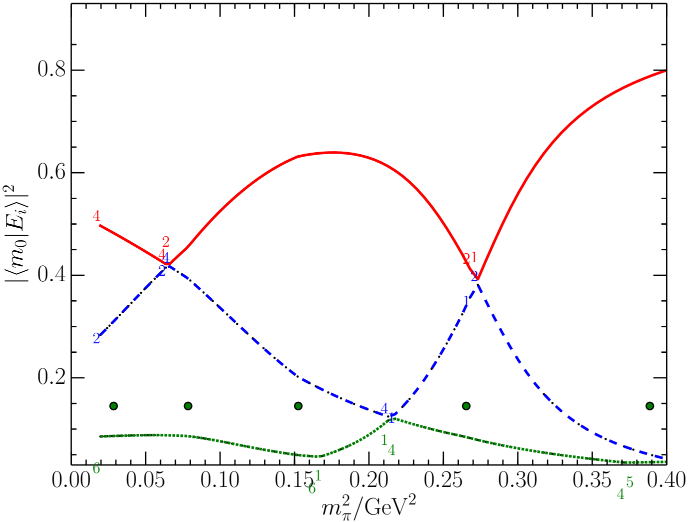

Bare State Strength in the N' Spectrum: 3 fm

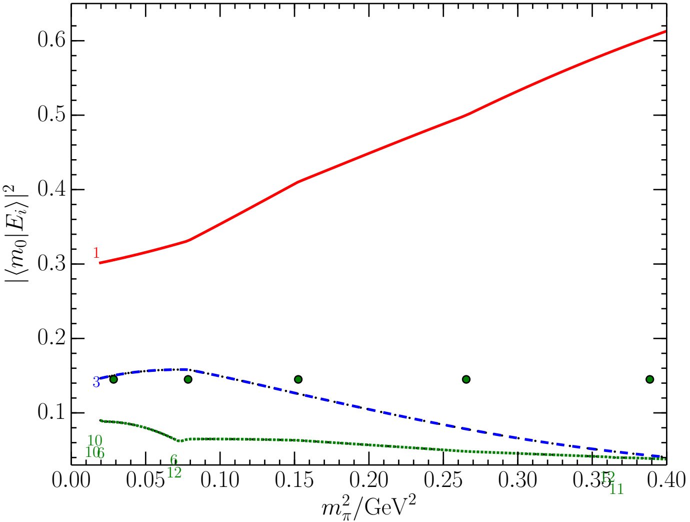

Volume Dependence of the N^* Spectrum

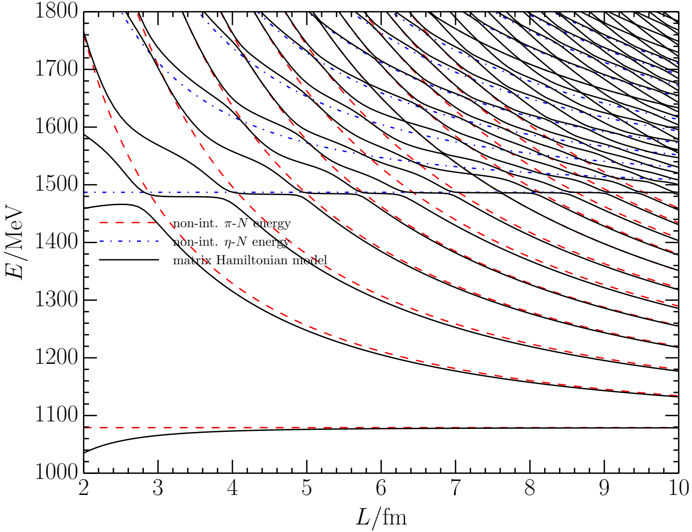

Volume Dependence of the N^* Spectrum

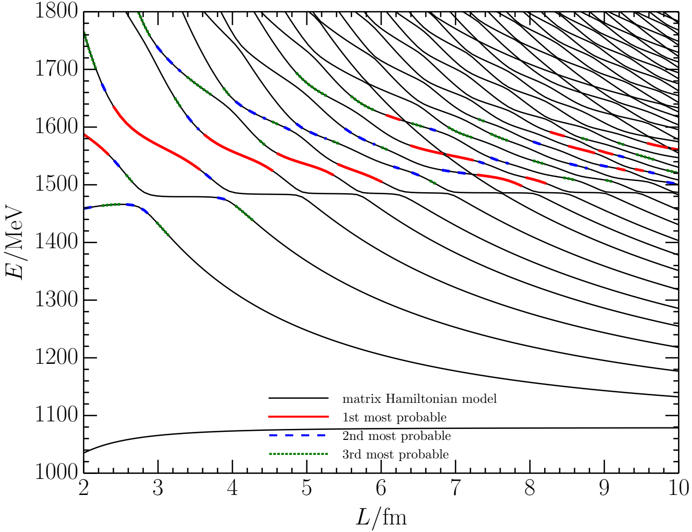

Basis Interpolator Superposition for Nucleon Spectrum

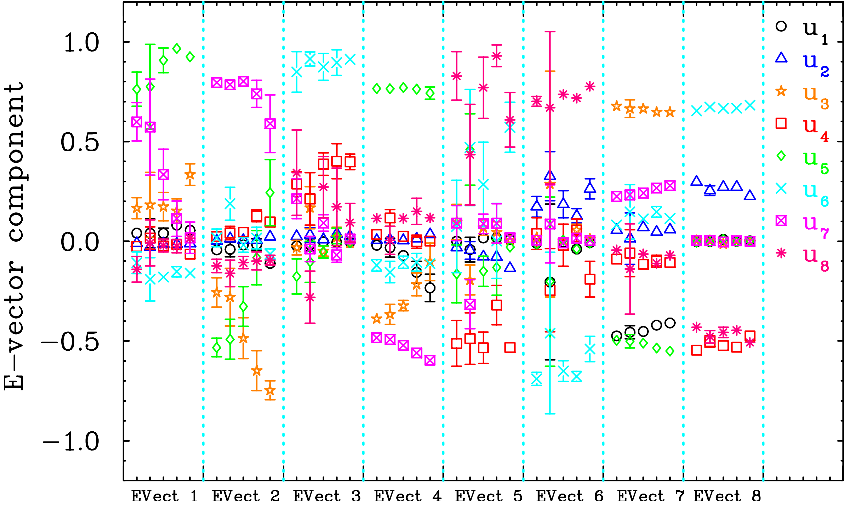

Artistic view of $\Lambda(1405)$ Structure

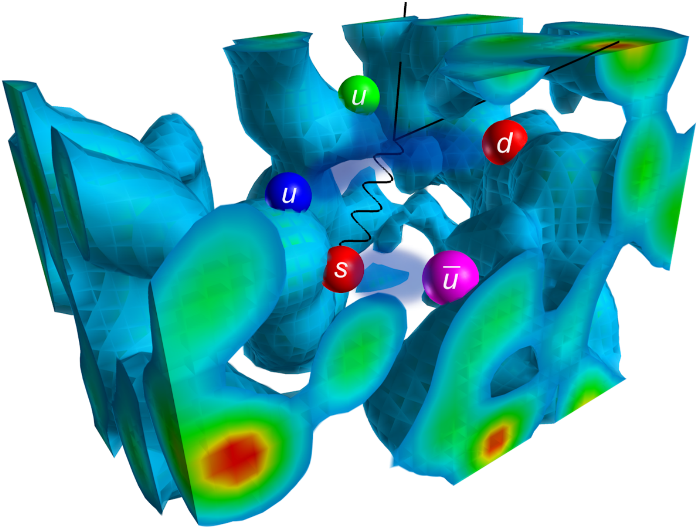

Operators Used in Λ(1405) Analysis

We consider local three-quark operators with the correct quantum numbers for the Λ channel, including

- Flavour-octet operators

$$\chi_1^8 = \frac{1}{\sqrt{6}}\varepsilon^{abc}\left(2(u^a C\gamma_5 d^b)s^c + (u^a C\gamma_5 s^b)d^c - (d^a C\gamma_5 s^b)u^c\right)$$
$$\chi_2^8 = \frac{1}{\sqrt{6}}\varepsilon^{abc}\left(2(u^a C d^b)\gamma_5 s^c + (u^a C s^b)\gamma_5 d^c - (d^a C s^b)\gamma_5 u^c\right)$$

- Flavour-singlet operator

$$\chi^1 = 2\varepsilon^{abc}\left((u^a C\gamma_5 d^b)s^c - (u^a C\gamma_5 s^b)d^c + (d^a C\gamma_5 s^b)u^c\right)$$

Operators Used in $\Lambda(1405)$ Analysis

We also use gauge-invariant Gaussian smearing to increase our operator basis.

- These results use 16 and 100 sweeps.
  - Gives a 6×6 matrix.

Operators Used in $\Lambda(1405)$ Analysis

We also use gauge-invariant Gaussian smearing to increase our operator basis.

- These results use 16 and 100 sweeps.
  - Gives a 6×6 matrix.
- Also considered 35 and 100 sweeps.
  - Results are consistent with larger statistical uncertainties.

Flavour structure of the $\Lambda(1405)$

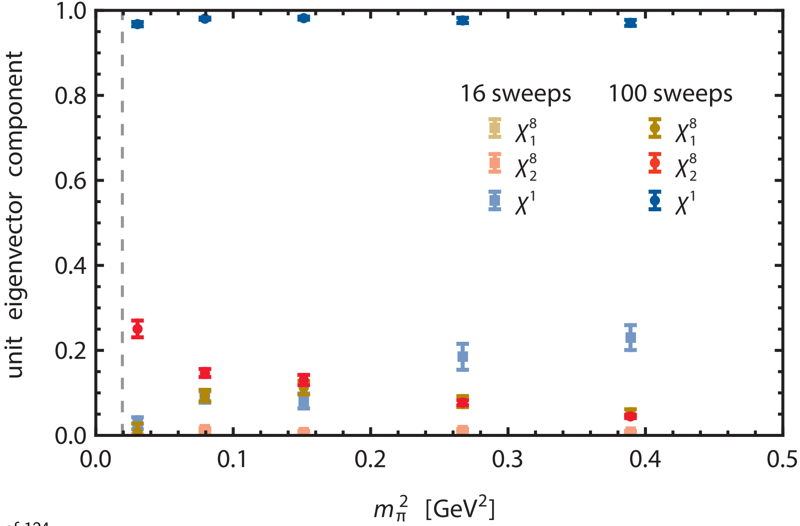

Volume dependence of the odd-parity Λ spectrum

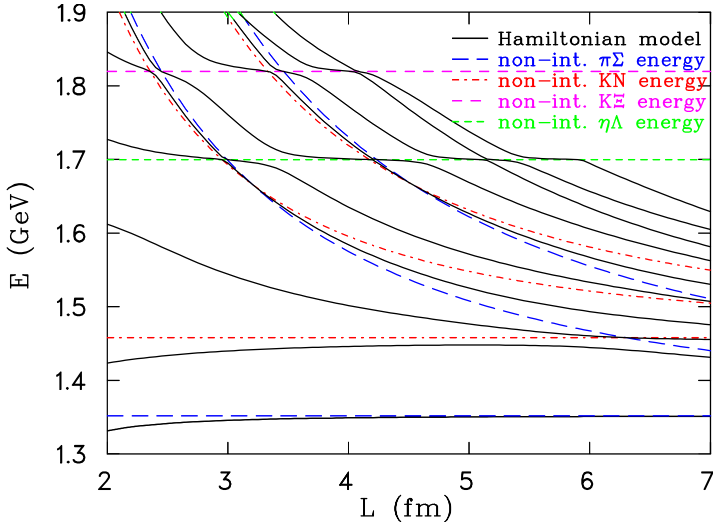

Infinite-volume reconstruction of the Λ(1405) energy

- Bootstraps are calculated by altering the value of each lattice data point by a Gaussian-distributed random number, weighted by the uncertainty.

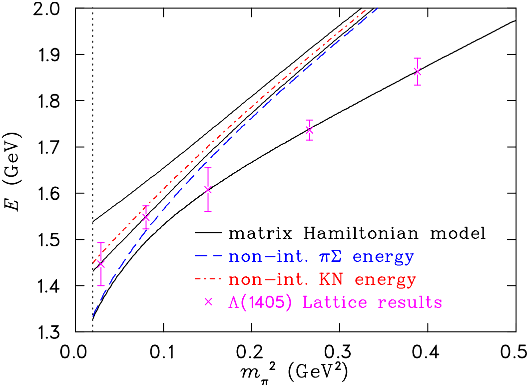

Infinite-volume $\Lambda(1405)$ mass distribution at m_π^{phys}

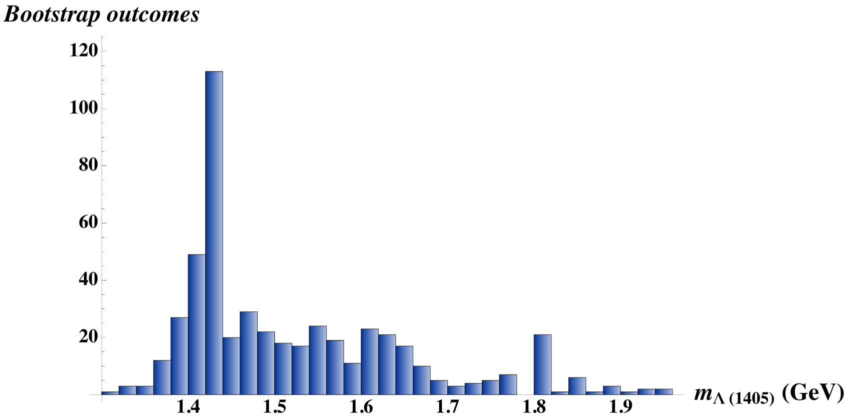

Dispersion Relation Test for the Λ(1405)

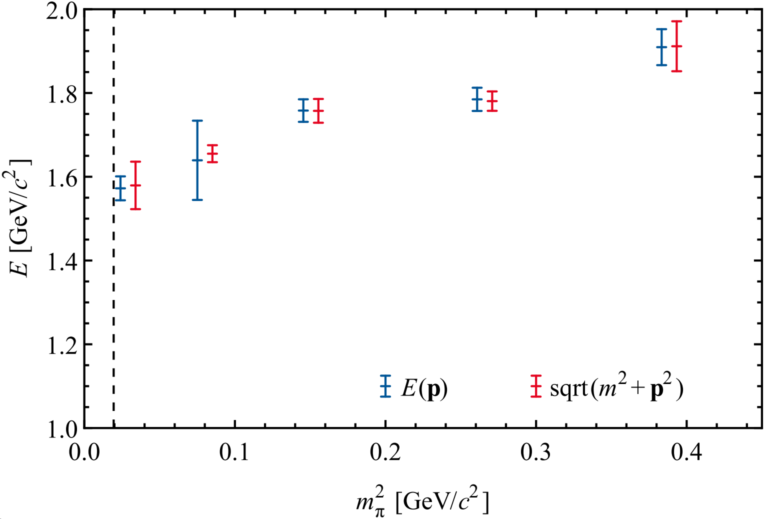

$\mathcal{G}_\mathrm{E}$ for the $\Lambda(1405)$

When compared to the ground state, the results for $\mathcal{G}_\mathrm{E}$ are consistent with the development of a non-trivial $\overline{\mathrm{K}}\mathrm{N}$ component at light quark masses.

$\mathcal{G}_{\mathsf{E}}$ for the $\Lambda(1405)$

When compared to the ground state, the results for $\mathcal{G}_{\mathsf{E}}$ are consistent with the development of a non-trivial $\overline{\mathrm{K}}$N component at light quark masses.

- Noting that the centre of mass of the $\overline{K}(s, \bar{\ell})\ N(\ell, u, d)$ is nearer the heavier N,
  - The anti–light-quark contribution, $\bar{\ell}$, is distributed further out by the $\overline{\mathrm{K}}$ and leaves an enhanced light-quark form factor.

$\mathcal{G}_E$ for the $\Lambda(1405)$

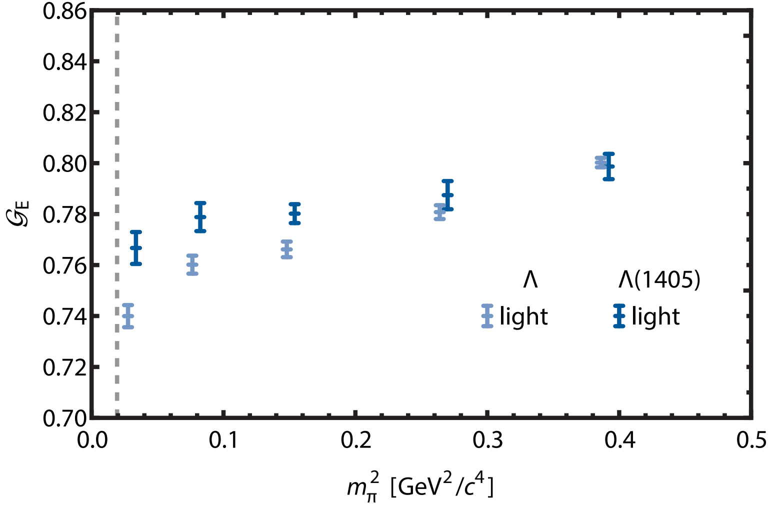

$\mathcal{G}_{\mathrm{E}}$ for the $\Lambda(1405)$

When compared to the ground state, the results for $\mathcal{G}_{\mathrm{E}}$ are consistent with the development of a non-trivial $\overline{\mathrm{K}}\mathrm{N}$ component at light quark masses.

- Noting that the centre of mass of the $\overline{K}(s,\bar{\ell})\ N(\ell,u,d)$ is nearer the heavier N,
  - The anti–light-quark contribution, $\bar{\ell}$, is distributed further out by the $\overline{\mathrm{K}}$ and leaves an enhanced light-quark form factor.
  - The strange quark may be distributed further out by the $\overline{\mathrm{K}}$ and thus have a smaller form factor.

$\mathcal{G}_E$ for the $\Lambda(1405)$

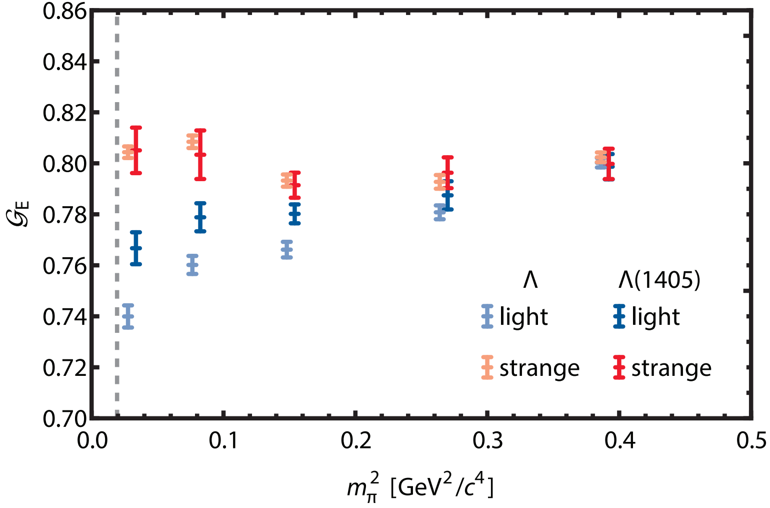

Hamiltonian model, H_I

- The form of the interaction is derived from chiral effective field theory.

$$g_{MB}(k_n) = \left(\frac{\kappa_{MB}}{16\pi^2 f_\pi^2} \frac{C_3(n)}{4\pi} \left(\frac{2\pi}{L}\right)^3 \omega_M(k_n)\, u^2(k_n) \right)^{1/2} .$$

- κ_{MB} denotes the $SU(3)$-flavour singlet couplings

$$\kappa_{\pi\Sigma} = 3\xi_0, \qquad \kappa_{\bar{K}N} = 2\xi_0, \qquad \kappa_{K\Xi} = 2\xi_0, \qquad \kappa_{\eta\Lambda} = \xi_0,$$

with $\xi_0 = 0.75$ reproducing the physical $\Lambda(1405) \to \pi\Sigma$ width.

Hamiltonian model, H_I

- The form of the interaction is derived from chiral effective field theory.

$$g_{MB}(k_n) = \left(\frac{\kappa_{MB}}{16\pi^2 f_\pi^2} \frac{C_3(n)}{4\pi} \left(\frac{2\pi}{L}\right)^3 \omega_M(k_n)\, u^2(k_n) \right)^{1/2} .$$

- κ_{MB} denotes the $SU(3)$-flavour singlet couplings

$$\kappa_{\pi\Sigma} = 3\xi_0, \qquad \kappa_{\bar{K}N} = 2\xi_0, \qquad \kappa_{K\Xi} = 2\xi_0, \qquad \kappa_{\eta\Lambda} = \xi_0,$$

  with $\xi_0 = 0.75$ reproducing the physical $\Lambda(1405) \to \pi\Sigma$ width.
- $C_3(n)$ is a combinatorial factor equal to the number of unique permutations of the momenta indices $\pm n_x$, $\pm n_y$ and $\pm n_z$.

Hamiltonian model, H_I

- The form of the interaction is derived from chiral effective field theory.

$$g_{MB}(k_n) = \left(\frac{\kappa_{MB}}{16\pi^2 f_\pi^2} \frac{C_3(n)}{4\pi} \left(\frac{2\pi}{L}\right)^3 \omega_M(k_n)\, u^2(k_n) \right)^{1/2} .$$

- κ_{MB} denotes the $SU(3)$-flavour singlet couplings

$$\kappa_{\pi\Sigma} = 3\xi_0, \qquad \kappa_{\bar{K}N} = 2\xi_0, \qquad \kappa_{K\Xi} = 2\xi_0, \qquad \kappa_{\eta\Lambda} = \xi_0,$$

  with $\xi_0 = 0.75$ reproducing the physical $\Lambda(1405) \to \pi\Sigma$ width.
- $C_3(n)$ is a combinatorial factor equal to the number of unique permutations of the momenta indices $\pm n_x$, $\pm n_y$ and $\pm n_z$.
- $u(k_n)$ is a dipole regulator, with regularization scale $\Lambda = 0.8$ GeV.

Infinite-volume reconstruction of the Λ(1405) energy

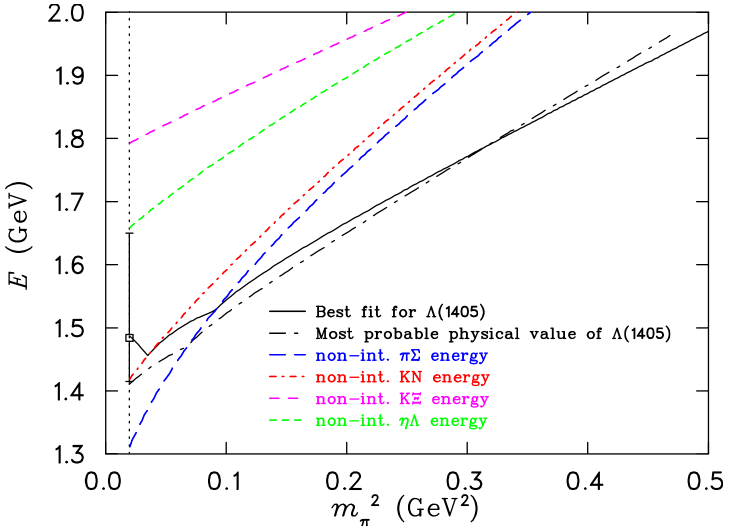

Excited State Form Factors

- The eigenstate-projected three-point correlation function is

$$G^{\mu}_{\alpha}(\mathbf{p}', \mathbf{p}; t_2, t_1) = \sum_{\mathbf{x}_1,\, \mathbf{x}_2} \mathrm{e}^{-\mathrm{i}\,\mathbf{p}'\cdot\mathbf{x}_2} \mathrm{e}^{\mathrm{i}(\mathbf{p}'-\mathbf{p})\cdot\mathbf{x}_1} \times$$

$$\times \langle\Omega| v^{\alpha}_{i}(\mathbf{p}')\, \chi_i(x_2)\, j^{\mu}(x_1)\, \overline{\chi}_j(0)\, u^{\alpha}_{i}(\mathbf{p}) |\Omega\rangle$$

$$= \mathbf{v}^{\alpha\,\mathsf{T}}(\mathbf{p}')\, G^{\mu}_{ij}(\mathbf{p}', \mathbf{p}; t_2, t_1)\, \mathbf{u}^{\alpha}(\mathbf{p})$$

where

$$G^{\mu}_{ij}(\mathbf{p}', \mathbf{p}; t_2, t_1) = \sum_{\mathbf{x}_1,\, \mathbf{x}_2} \mathrm{e}^{-\mathrm{i}\,\mathbf{p}'\cdot\mathbf{x}_2} \mathrm{e}^{\mathrm{i}(\mathbf{p}'-\mathbf{p})\cdot\mathbf{x}_1} \langle\Omega| \chi_i(x_2)\, j^{\mu}(x_1)\, \overline{\chi}_j(0) |\Omega\rangle$$

is the matrix constructed from the three-point correlation functions of the original operators $\{\, \chi_i \,\}$.

Extracting Form Factors from Lattice QCD

- To eliminate the time dependence of the three-point correlation function, we construct the ratio

$$R^{\mu}_{\alpha}(\mathbf{p}', \mathbf{p}; t_2, t_1) = \left(\frac{G^{\mu}_{\alpha}(\mathbf{p}', \mathbf{p}; t_2, t_1)\, G^{\mu}_{\alpha}(\mathbf{p}, \mathbf{p}'; t_2, t_1)}{G_{\alpha}(\mathbf{p}'; t_2)\, G_{\alpha}(\mathbf{p}; t_2)} \right)^{1/2}$$

Extracting Form Factors from Lattice QCD

- To eliminate the time dependence of the three-point correlation function, we construct the ratio

$$R^{\mu}_{\alpha}(\mathbf{p}', \mathbf{p}; t_2, t_1) = \left(\frac{G^{\mu}_{\alpha}(\mathbf{p}', \mathbf{p}; t_2, t_1)\, G^{\mu}_{\alpha}(\mathbf{p}, \mathbf{p}'; t_2, t_1)}{G_{\alpha}(\mathbf{p}'; t_2)\, G_{\alpha}(\mathbf{p}; t_2)} \right)^{1/2}$$

- To further simply things, we define the reduced ratio

$$\overline{R}^{\mu}_{\alpha} = \left(\frac{2E_{\alpha}(\mathbf{p})}{E_{\alpha}(\mathbf{p}) + m_{\alpha}} \right)^{1/2} \left(\frac{2E_{\alpha}(\mathbf{p}')}{E_{\alpha}(\mathbf{p}') + m_{\alpha}} \right)^{1/2} R^{\mu}_{\alpha}$$

Current Matrix Element for Spin-1/2 Baryons

The current matrix element for spin-1/2 baryons has the form

$$\langle p', s' | j^\mu | p, s \rangle = \left(\frac{m_\alpha^2}{E_\alpha(\mathbf{p}) E_\alpha(\mathbf{p}')} \right)^{1/2} \times$$

$$\times \, \overline{u}(\mathbf{p}') \left(F_1(q^2)\, \gamma^\mu + \mathrm{i}\, F_2(q^2)\, \sigma^{\mu\nu} \frac{q^\nu}{2m_\alpha} \right) u(\mathbf{p})$$

Current Matrix Element for Spin-1/2 Baryons

The current matrix element for spin-1/2 baryons has the form

$$\langle p', s' | j^\mu | p, s \rangle = \left(\frac{m_\alpha^2}{E_\alpha(\mathbf{p}) E_\alpha(\mathbf{p}')} \right)^{1/2} \times$$
$$\times \, \overline{u}(\mathbf{p}') \left(F_1(q^2)\, \gamma^\mu + \mathrm{i}\, F_2(q^2)\, \sigma^{\mu\nu} \frac{q^\nu}{2m_\alpha} \right) u(\mathbf{p})$$

- The Dirac and Pauli form factors are related to the Sachs form factors through

$$\mathcal{G}_\mathrm{E}(q^2) = F_1(q^2) - \frac{q^2}{(2m^\alpha)^2} F_2(q^2)$$
$$\mathcal{G}_\mathrm{M}(q^2) = F_1(q^2) + F_2(q^2)$$

Sachs Form Factors for Spin-1/2 Baryons

- A suitable choice of momentum ($\mathbf{q} = (q, 0, 0)$) and the (implicit) Dirac matrices allows us to directly access the Sachs form factors:
  - for $\mathcal{G}_{\mathrm{E}}$: using $\Gamma_4^{\pm}$ for both two- and three-point,

$$\mathcal{G}_{\mathrm{E}}^{\alpha}(q^2) = \overline{R}_{\alpha}^{4}(\mathbf{q}, \mathbf{0}; t_2, t_1)$$

  - for $\mathcal{G}_{\mathrm{M}}$: using $\Gamma_4^{\pm}$ for two-point and $\Gamma_j^{\pm}$ for three-point,

$$|\varepsilon_{ijk}\, q^i|\, \mathcal{G}_{\mathrm{M}}^{\alpha}(q^2) = (E_{\alpha}(\mathbf{q}) + m_{\alpha})\, \overline{R}_{\alpha}^{k}(\mathbf{q}, \mathbf{0}; t_2, t_1)$$

  - where for positive parity states,

$$\Gamma_j^{+} = \frac{1}{2}\begin{bmatrix} \sigma_j & 0 \\ 0 & 0 \end{bmatrix} \qquad \Gamma_4^{+} = \frac{1}{2}\begin{bmatrix} \mathbb{I} & 0 \\ 0 & 0 \end{bmatrix}$$

    and for negative parity states,

$$\Gamma_j^{-} = -\gamma_5 \Gamma_j^{+} \gamma_5 = -\frac{1}{2}\begin{bmatrix} 0 & 0 \\ 0 & \sigma_j \end{bmatrix} \qquad \Gamma_4^{-} = -\gamma_5 \Gamma_4^{+} \gamma_5 = -\frac{1}{2}\begin{bmatrix} 0 & 0 \\ 0 & \mathbb{I} \end{bmatrix}$$

Scattering State Contamination in Projected Correlator: CSSM

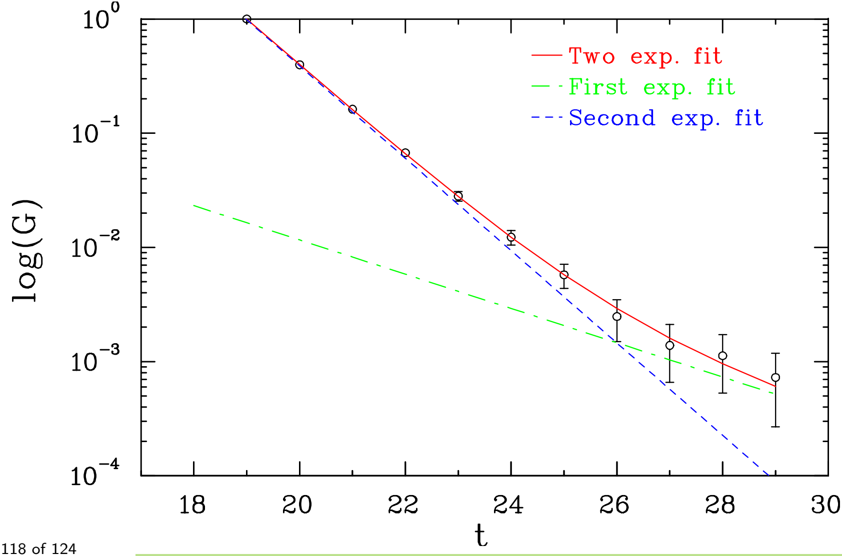

Negative Parity Nucleon: Five-quark Operators: CSSM

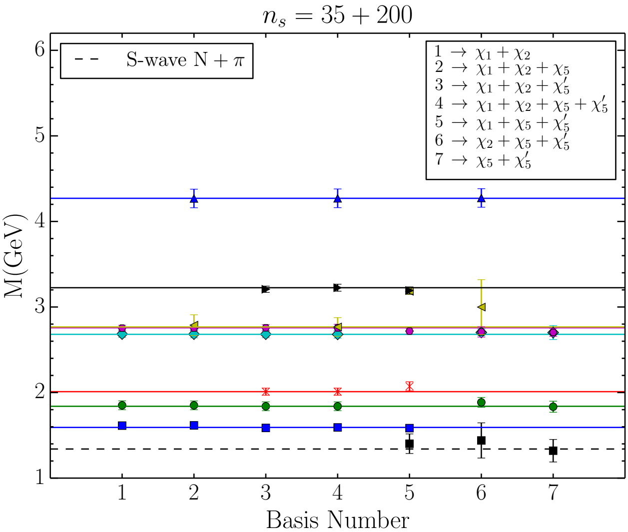

Negative Parity Nucleon Scattering Thresholds

- “Searching for low-lying multi-particle thresholds in lattice spectroscopy,”
  M. S. Mahbub, *et al.* [CSSM],
  Annals Phys. **342**, 270 (2014)
  arXiv:1310.6803 [hep-lat]

- “Lattice baryon spectroscopy with multi-particle interpolators,”
  Adrian Kiratidis, Waseem Kamleh, Derek Leinweber, Benjamin Owen [CSSM]
  Phys. Rev. D **91**, 094509 (2015)
  arXiv:1501.07667 [hep-lat].

Negative Parity Nucleon Spectrum: Lang and Verduci

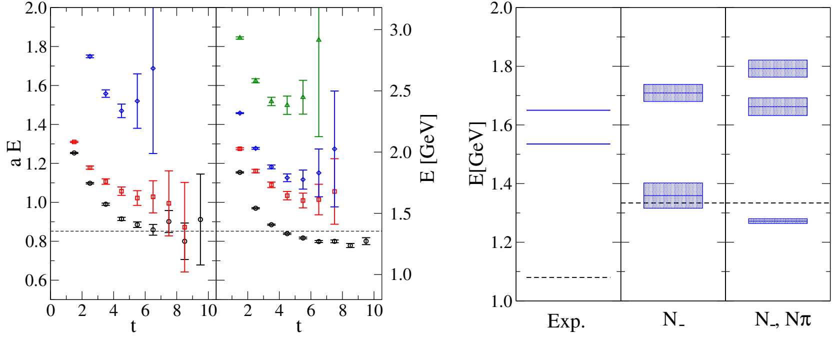

Negative Parity Nucleon Spectrum: Lang and Verduci

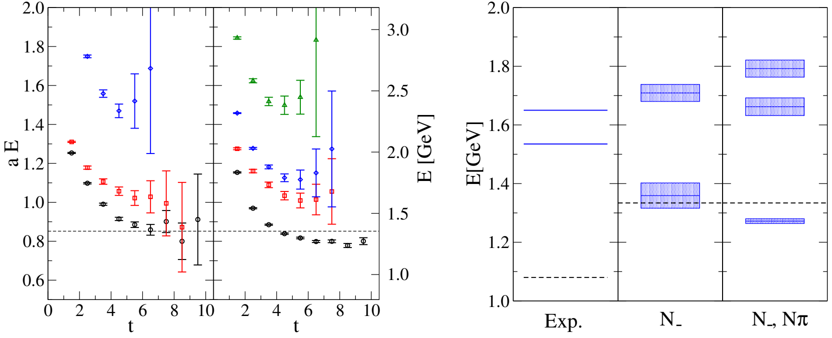

- Small correlation matrix: $\chi_1 + \chi_2 \times 2$ smearings $= 4 \times 4$

Negative Parity Nucleon Spectrum: Lang and Verduci

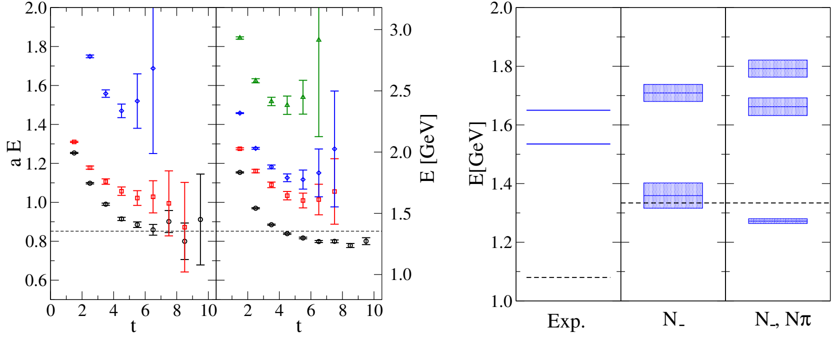

- Small correlation matrix: $\chi_1 + \chi_2 \times 2$ smearings $= 4 \times 4$
- Did not construct projected correlators.
- Limited Euclidean time evolution prior to ill conditioning.

Negative Parity Nucleon Spectrum: Lang and Verduci

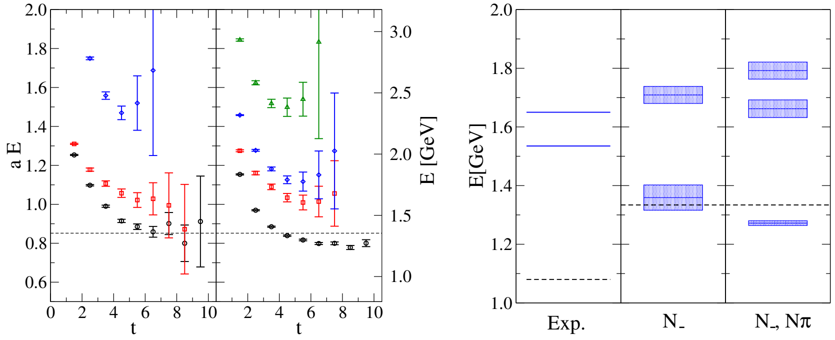

- Small correlation matrix: $\chi_1 + \chi_2 \times 2$ smearings $= 4 \times 4$
- Did not construct projected correlators.
- Limited Euclidean time evolution prior to ill conditioning.
- Adding $N\pi$ sufficient but not necessary. *cf.* Cypress Results...

Common Proton Interpolating Fields

- Many groups (BGR, Cypress, χQCD, CSSM) consider the following local interpolating fields

$$\chi_1(x) = \epsilon^{abc}(u^{Ta}(x)\, C\gamma_5\, d^b(x))\, u^c(x)\,,$$

$$\chi_2(x) = \epsilon^{abc}(u^{Ta}(x)\, C\, d^b(x))\,\gamma_5\, u^c(x)\,.$$

d-quark density in 1st excited state of proton: Lower Dirac Component

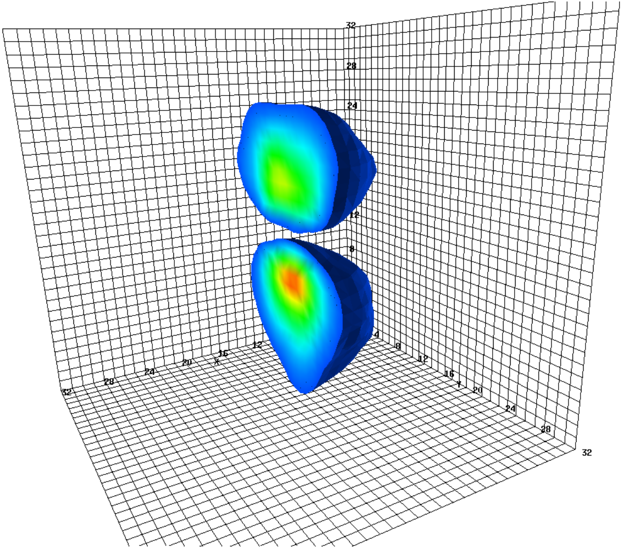

Hybrid Baryons: Hadron Spectrum Collaboration